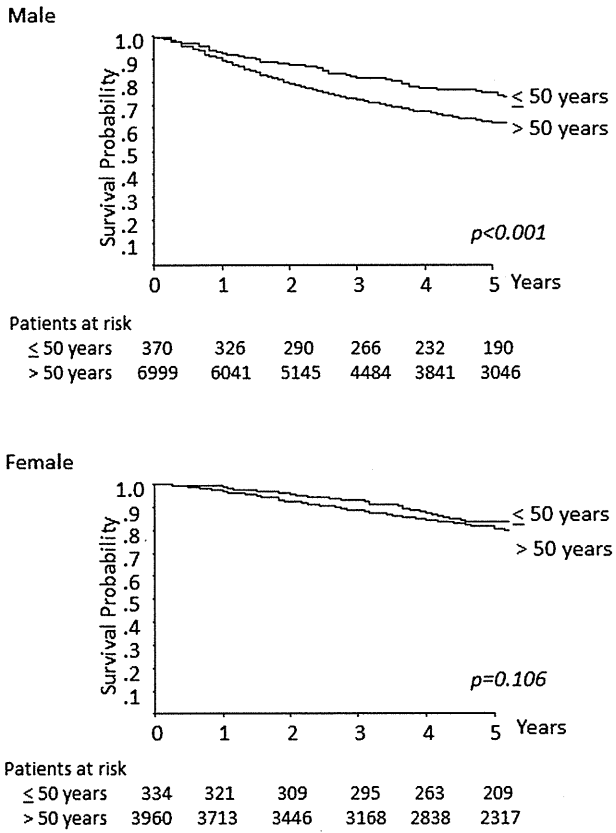

Fig. 3. The survival curves of patients aged up to and older than 50 years with surgery according to sex. Among male patients, the overall survival in patients aged up to 50 years was significantly better than that in patients older than 50 years. No significant difference was found in female patients.

were also performed. The 5Y-OS was 79.2% and 73.7% in the young and young elderly groups, respectively ($p = 0.002$). According to p-stage, the 5Y-OS was 94.8% and 90.6% for IA ($p = 0.022$), 87.0% and 79.0% for IB ($p = 0.027$), 61.0% and 66.9% for IIA, 71.0% and 54.7% for IIB ($p = 0.027$), 49.6% and 44.7% for IIIA, and 80.0% and 27.7% for IIIB ($p = 0.023$), in the young and young elderly groups, respectively. These differences showed a similar tendency to have a better survival rate in the young group as seen with the comparative results between those aged up to and those older than 50 years shown above. However, survival after postoperative recurrence did not show a significant difference between the young and young elderly groups.

The prognostic factors were tested by multivariate analyses using the variables of age, sex, ECOG-PS, smoking history, comorbidity, operative procedure, p-stage, histology, adjuvant therapy (Table 2). Age up to 50 years was identified to be an independent prognostic factor with a hazard ratio of 1.451. Female, good ECOG-PS, no smoking history, no comorbidity, early p-stage, and no preoperative adjuvant therapy were also identified as predictors of a better prognosis. When analyzing age as continuous variable in multivariate analysis, age was identified as an independent prognostic factor with the hazard ratio 1.026 (CI: 1.022–1.030).

4. Discussion

The postoperative survival of young lung cancer patients remains unclear due to their low numbers, though several studies have been reported so far [3–10]. Radzikowska et al. and Minami et al. investigated patients younger than 50 years and showed significantly better survival as compared to old patients [4,6]. Among several studies with definition of the young group as up to 40 years, Tian et al. reported higher 5Y-OS in young patients, though no superior survival was shown in the study by Hanagiri et al. or by Maruyama et al. [5,7,8]. In the present epidemiological study, cancer patients aged up to 50 years who underwent surgery were extracted from the Japanese Lung Cancer Registry Study 2004 [2],

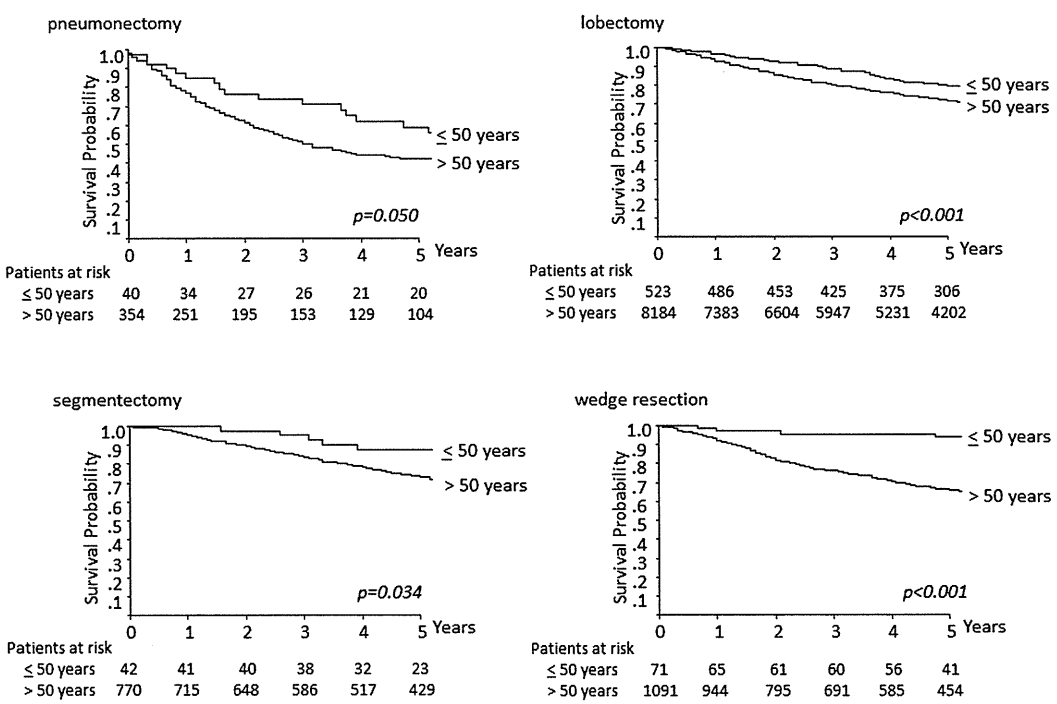

Fig. 4. The survival curves of patients aged up to and older than 50 years with surgery according to operative procedure. The postoperative survival was significantly better in the young group for each procedure.

Table 1
Patients' characteristics.

	Age ≤ 50 years	Age > 50years	p value
Sex			p < 0.001
Male	370(52.6%)	6999(63.2%)	
Female	334(47.4%)	3960(36.8%)	
PS			p < 0.001
0	665(94.5%)	8943(81.6%)	
1	27(3.8%)	1661(15.1%)	
Others	12(1.7%)	355(3.3%)	
Smoking history			p < 0.001
No	308(43.8%)	3777(34.5%)	
Yes	334(47.4%)	6290(57.4%)	
Unknown	62(8.8%)	892(8.1%)	
Comorbidity			p < 0.001
No	562(79.8%)	7151(65.3%)	
Yes	79(11.2%)	3048(27.8%)	
Unknown	63(8.9%)	760(6.9%)	
c-stage			p < 0.001
Stage IA	420(59.7%)	5875(53.6%)	
Stage IB	88(12.5%)	2700(24.6%)	
Stage IIA	36(5.1%)	167(1.5%)	
Stage IIB	45(6.4%)	854(7.8%)	
Stage IIIA	84(11.9%)	856(7.8%)	
Stage IIIB	13(1.8%)	394(3.6%)	
Stage IV	18(2.6%)	113(1.0%)	
Operative procedure			p < 0.001
Pneumonectomy	40(5.7%)	354(3.2%)	
Bilobectomy	18(2.6%)	357(3.3%)	
Lobectomy	523(74.3%)	8184(74.7%)	
Segmentectomy	42(6.0%)	770(7.0%)	
Wedge resection	71(10.1%)	1091(10.0%)	
Others	10(1.3%)	203(1.9%)	
p-stage			p < 0.001
Stage IA	331(47.0%)	4647(42.4%)	
Stage IB	119(16.9%)	2433(22.2%)	
Stage IIA	39(5.5%)	902(8.2%)	
Stage IIB	49(7.0%)	799(7.3%)	
Stage IIIA	128(18.2%)	1676(15.3%)	
Stage IIIB	6(0.9%)	100(0.9%)	
Stage IV	32(4.5%)	402(3.7%)	
Histology			p < 0.001
Adenocarcinoma	554(78.7%)	7367(67.2%)	
Squamous cell carcinoma	52(7.4%)	2548(23.3%)	
Large cell carcinoma	30(4.3%)	357(3.3%)	
Small cell carcinoma	11(1.6%)	232(2.1%)	
Others	57(8.0%)	455(4.1%)	
Preoperative adjuvant therapy			p < 0.001
Yes	73(10.4%)	520(4.7%)	
No	631(89.6%)	10,439(95.3%)	
Postoperative adjuvant therapy			p < 0.001
Yes	221(31.4%)	2682(24.5%)	
No	483(68.6%)	8277(75.5%)	
Total	704(100%)	10,959(100%)	

PS, Eastern Cooperative Oncology Group performance status; Smoking history, including both current and ex-smokers; Comorbidity, including current smoking history, obesity with BMI > 30 kg/m^2, cerebrovascular disease, chronic obstructive pulmonary disease, interstitial pneumonia, ischemic heart disease, renal dysfunction with creatinine> 2.0 g/dL, liver cirrhosis with Child-Turcotte classification > B, diabetes mellitus with HbA1c > 8%, anemia with Hb < 8 g/dL, and treatment for other malignancy within a year.

Table 2
Results of multivariate analysis in lung cancer patients with surgical resection.

Variables		Hazard ratio	95% Confidence Interval	p value
Age				
≤50 years		1.000		
>50 years		1.451	1.211–1.739	<0.001
Sex				
Male		1.000		
Female		0.664	0.593–0.744	<0.001
ECOG PS				
PS 0		1.000		
PS 1		1.582	1.441–1.736	<0.001
PS 2		2.041	1.600–2.604	<0.001
PS 3		2.706	1.717–4.266	<0.001
Smoking history				
No		1.000		
Yes		1.150	1.026–1.289	0.016
Comorbidity				
No		1.000		
Yes		1.232	1.135–1.338	<0.001
Operative procedure				
Pneumonectomy		1.000		
Bilobectomy		1.089	0.873–1.358	0.450
Lobectomy		0.782	0.665–0.920	0.003
Segmentectomy		0.978	0.786–1.218	0.844
p-stage				
IA		1.000		
IB		1.958	1.741–2.203	<0.001
IIA		2.878	2.488–3.329	<0.001
IIB		4.031	3.505–4.637	<0.001
IIIA		6.940	5.288–9.108	<0.001
Histology				
Pre-invasive lesion		1.000		
Squamous cell carcinoma		1.280	0.318–5.151	0.728
Small cell carcinoma		1.961	0.481–7.994	0.348
Adenocarcinoma		1.166	0.291–4.682	0.828
Large cell carcinoma		1.721	0.425–6.978	0.447
Adjuvant therapy				
Preoperative	No	1.000		
	Yes	1.169	1.018–1.342	0.027
Postoperative	No	1.000		
	Yes	0.923	0.850–1.002	0.055

ECOG, Eastern Cooperative Oncology Group; PS, Performance Status; Adjuvant therapy includes systemic chemotherapy and radiation therapy.

and better postoperative survival was observed in these young lung cancer patients, although the proportion of advance disease was higher as compared to the old group. It was also found that, among young patients, women and those with adenocarcinoma had a better survival, which was similar to the results of all-generation analyses [2].

The higher proportion of young patients who underwent pneumonectomy could imply that they were better able to tolerate surgery, as a previous report showed similar results [5]. Pneumonectomy was, however, reported to increase the perioperative morbidity in elderly patients in a case-control study [11], and sleeve lobectomy, if possible, is recommended as an alternative procedure to pneumonectomy, with lower mortality and better survivals [12].

The results of the present study might indicate the importance given to curative intention over the preservation of pulmonary function in young patients. The superior 5Y-OS in young group treated with a pneumonectomy in the present study could suggest that pneumonectomy is still a considerable option for resectable locally advanced disease in the young patients.

Higher rates of both preoperative and postoperative adjuvant therapy in the young group could reflect the higher proportion of stage IIIA advanced disease, which is a prime indication for induction therapy [13], in addition to the ability of young patients to tolerate such treatment. Radzikowska et al. also reported similar results with more aggressive treatment in young patients [4]. The rate of preoperative adjuvant therapy in the young group was more than 2-fold that in those old group (Table 1). These results indicate a planned active multimodal strategy in young patients with good performance status, while the clinical effect to the survival is unclear. Since postoperative adjuvant chemotherapy was adopted as an evidence-based treatment in a practice guideline for lung cancer treatment in 2005 in Japan, quoting several meta-analyses and randomized studies [14–17], only a proportion of patients with stage IB-IIIA analyzed in the present study had received adjuvant therapy. Thus, it might be expected that postoperative survival in patients with locally advanced disease has potentially become better with postoperative chemotherapy, though further investigation is necessary to identify the issue.

The overall survival rates for patients with stages IA, IB, IIB, IIIA, and IIIB were better for patients aged up to 50 years than for

patients older than 50 years. We added another comparison of survival between patients aged up to 50 years and those 50–70 years, because it is expected that patients older than 70 years could have more frequent lung cancer-unrelated death. The similar results to the comparison between patients aged up to and older than 50 years might suggest other factors in addition to the natural aging bias. Though we could not analyze the treatment after recurrence in the present study, young patients with good performance status might have more chance to receive second and third lines of chemotherapy. Further investigation is required to clarify the clinical impact on survival of the aggressive multimodality therapy in young patients with postoperative recurrence using recent cases.

The worse postoperative survival in males older than 50 years was probably due to the greater number of lung cancer-unrelated deaths in that group. This cohort with more comorbidities and smoking history could have cardiopulmonary diseases or second primary malignancies related to tobacco exposure. The poor general status of the old patients might also be related to the less frequent use of adjuvant therapies. As a result, the young male patients without comorbidity or smoking history might improve the survival of the entire patient group. The death rate of male is reported to be twice higher than that of female in 30–84 year-old population by Statistics and Information Department, Minister's Secretariat, Ministry of Health, Labor and Welfare, Japan. Thus, such natural biological bias might also influence to the results.

The tendency for favorable survival in female patients and in patients with adenocarcinoma histology was the same as that seen with all-generation analyses [2]. Bronchioloalveolar carcinoma (BAC) showing ground glass opacity on CT scanning, which is currently classified as adenocarcinoma in situ or minimally invasive adenocarcinoma [18], is generally recognized to be a slow growing, low-grade adenocarcinoma and a unique subtype related to a never-smoking history, female sex, and Asian race [19]. Though CT findings were not analyzed in the present study cohort, higher proportions of adenocarcinoma and females in the Japanese young patients' group might change the patients' characteristics, with a higher rate of BAC and low-grade malignant behavior. Further investigations including CT findings are necessary to resolve these issues.

The present epidemiological study has several limitation and speculation for the results. The retrospective study cannot clarify the prognostic effect of multimodal therapy in young patients due to the lack of data for chemotherapy regimens or molecular target therapy. Younger age is well-known better prognostic predictor in other malignancies and the influence of other factors except the variables analyzed in this study cannot be completely denied. Further prospective analyses using high volume surgically and non-surgically treated lung cancer patients are required to clarify the cause for the better prognosis of young patients treated surgically.

5. Conclusion

In conclusion, surgically treated young lung cancer patients showed the highest rate of locally advanced disease and received active multimodality therapies. Their postoperative survival was better than that of patients older than 50 years, and age was identified as an independent better prognostic factor. Even when comparing cancer-related survival, the outcome was significantly better in young lung cancer patients.

Conflict of interest statement

All authors contributing to this work have no other conflict of interest to declare.

References

[1] Lung Cancer. American Cancer Society; 2013. Available at: http://www.cancer.org/Cancer/ [accessed 22.01.13].
[2] Sawabata N, Miyaoka E, Asamura H, Nakanishi Y, Eguchi K, Mori M, et al. Japanese lung cancer registry study of 11,663 surgical cases in 2004: demographic and prognosis changes over decade. J Thorac Oncol 2011;6:1229–35.
[3] Zhang J, Chen S, Zhen Y, Xiang J, Wu C, Bao P, et al. Multicenter study of lung cancer patients younger than 45 years in Shanghai. Cancer 2010;116:3656–62.
[4] Radzikowska E, Roszkowski K, Glaz P. Lung cancer in patients under 50 years old. Lung Cancer 2001;33:203–11.
[5] Tian DL, Liu HX, Zhang L, Yin HN, Hu YX, Zhao HR, et al. Surgery for young patients with lung cancer. Lung Cancer 2003;42:215–20.
[6] Minami H, Yoshimura M, Matsuoka H, Toshihiko S, Tsubota N. Lung cancer treated surgically in patients <50 years of age. Chest 2001;120:32–6.
[7] Hanagiri T, Sugio K, Uramoto H, Sugaya M, Ono K, So T, et al. Results of surgical treatment for lung cancer in young adults. Int Surg 2008;93:50–4.
[8] Maruyama R, Yoshino I, Yohena T, Uehara T, Kanematsu T, Kitajima M, et al. Lung cancer in patients younger than 40 years of age. J Surg Oncol 2001;77:208–12.
[9] International Union against Cancer, Sobin LH, Gospodarowicz MK, Wittekind C, editors. TNM classification of malignant tumours. 7th ed. New York, NY: Wiley-Liss; 2009.
[10] Mauri D, Pentheroudakis G, Bafaloukos D, Pectasides D, Samantas E, Efstathiou E, et al. Non-small cell lung cancer in the young: a retrospective analysis of diagnosis, management and outcome data. Anticancer Res 2006;26:3175–81.
[11] Leo F, Scanagatta P, Baglio P, Radice D, Veronesi G, Solli P, et al. The risk of pneumonectomy over the age of 70. A case-control study. Eur J Cardiothorac Surg 2007;31:780–2.
[12] Park JS, Yang HC, Kim HK, Kim K, Shim YM, Choi YS, et al. Sleeve lobectomy as an alternative procedure to pneumonectomy for non-small cell lung cancer. J Thorac Oncol 2010;5:517–20.
[13] Non-Small Cell Lung Cancer. http://www.nccn.org/index.asp
[14] Arriagada R, Bergman B, Dunant A, Le Chevalier T, Pignon JP, Vansteenkiste J, et al. Cisplatin-based adjuvant chemotherapy in patients with completely resected non-small-cell lung cancer. N Engl J Med 2004;350:351–60.
[15] Hotta K, Matsuo K, Ueoka H, Kiura K, Tabata M, Tanimoto M. Role of adjuvant chemotherapy in patients with resected non-small-cell lung cancer: reappraisal with a meta-analysis of randomized controlled trials. J Clin Oncol 2004;22:3860–7.
[16] Winton T, Livingston R, Johnson D, Rigas J, Johnston M, Butts C, et al. Vinorelbine plus cisplatin vs. observation in resected non-small-cell lung cancer. N Engl J Med 2005;352:2589–97.
[17] Hamada C, Tanaka F, Ohta M, Fujimura S, Kodama K, Imaizumi M, et al. Meta-analysis of postoperative adjuvant chemotherapy with tegafur-uracil in non-small-cell lung cancer. J Clin Oncol 2005;23:4999–5006.
[18] Travis WD, Brambilla E, Noguchi M, Nicholson AG, Geisinger KR, Yatabe Y, et al. International association for the study of lung cancer/American thoracic society/European respiratory society international multidisciplinary classification of lung adenocarcinoma. J Thorac Oncol 2011;6:244–85.
[19] Raz DJ, Jablons DM. Bronchioloalveolar carcinoma is not associated with younger age at diagnosis: an analysis of the SEER database. J Thorac Oncol 2006;1:339–43.

In Response:

We appreciate the comments by Dr. Poullis regarding our recent study examining outcomes in patients with clinical stage IIIA(N2) non–small-cell lung cancer.

We agree that the elimination of patients who did not survive 4 months from the analysis was a limitation of the study. The use of Cox–Aalen regression may have mitigated this bias, however, it would not control for potential time biases because of differences in the duration of time it takes to complete certain treatment categories.[1]

Dr. Poullis states that there were several covariates affecting survival, such as age, laterality, and histology not included in the Cox regression analysis. In the Methods section we state that these variables were included in our model and were controlled by stratification because of the violation of proportional hazard for these variables. This allows for calculation of hazard ratio for those variables that do not violate the proportional hazard assumption but it does preclude the generation of hazard ratio estimates for variables that do violate the proportional hazard assumption. Therefore, covariates including age, laterality, and histology were included as covariates in the model; however, specific hazard ratios for each of these variables are unavailable.

Table 3 reveals an overlap between the confidence intervals for patients who underwent neoadjuvant + lobectomy versus lobectomy followed by adjuvant therapy. However, this table only included patients diagnosed in 2003–2004 (N = 4025) and the purpose of these results was to examine whether comorbidity significantly affected outcomes, which it did not. Our initial cohort with a larger number of patients (N = 10,058) revealed a significant difference in hazard ratios between the neoadjuvant + lobectomy and lobectomy followed by adjuvant therapy groups. We agree with Dr. Poulis that future studies will continue to clarify this issue.

Matthew Koshy, MD
Radiation and Cellular Oncology
University of Chicago
Chicago, IL

REFERENCE

1. Park HS, Gross CP, Makarov DV, Yu JB. Immortal time bias: a frequently unrecognized threat to validity in the evaluation of postoperative radiotherapy. *Int J Radiat Oncol Biol Phys* 2012.

Disclosure: The author declares no conflict of interest.

Address for correspondence: Matthew Koshy, MD, Radiation and Cellular Oncology University of Chicago, 5758 S. Maryland Avenue 9006, Chicago, IL 60637. E-mail: mkoshy@radonc.uchicago.edu

ISSN: 1556-0864/13/0811-0e101

Overdiagnosis in Lung Cancer Screening with Low-Dose Computed Tomography

To the Editor:

We congratulate Pegna et al.[1] for their very important contribution to the field of lung cancer screening by reporting the interim results of the Italian Lung (ITALUNG) trial, a randomized control study for lung cancer screening with low-dose computed tomography (LDCT) compared with usual care. On the basis of the evidence provided by the National Lung Screening Trial (NLST),[2] established guidelines, including one by the National Comprehensive Cancer Network, now recommend screening for lung cancer using LDCT in individuals with high risk. However, many issues remain to be solved before these research results can be extrapolated to community practice. This article provides clues to overcoming some of these issues, as it reports the feasibility of mail-based participant recruitment and a shared protocol for nodule management using follow-up CT, 2-fluoro-2-deoxy-D glucose-positron emission tomography, CT-guided fine-needle aspiration biopsy, and bronchoscopic biopsy. Lung cancer detection rates using LDCT are also discussed.

Among 1406 participants who were randomly allocated to the LDCT screening group and who completed the baseline screening, the authors detected 20 patients with lung tumors at baseline (detection rate of 1.5%) and an additional 18 patients during three annual subsequent screening rounds (detection rate of 0.5%). The detection rate was significantly higher for the baseline compared with the subsequent screening rounds, as has been similarly shown in other observational and randomized trials including the NLST; this result ostensibly seems reasonable because of the accumulated patients with lung cancer who are likely present at the baseline screening. However, this enhanced detection at baseline might also be attributed to other factors. For example, indolent cancers tend to accumulate preferentially without presenting symptoms, leading to a higher rate of overdiagnosis at baseline than during subsequent screening rounds. In fact, a total of 1060 and 941 patients with lung cancer were diagnosed in the CT and radiograph screening groups, respectively, in the NLST.[2] The difference between these two groups, that is, 119 patients, might reflect the occurrence of overdiagnosis. According to a recent publication[3] on the initial results of this trial, 292 and 190 patients were diagnosed as having lung cancer in the CT and radiograph screening groups during the first round of screening, respectively, resulting in a difference of 102 patients: as many as 86% (102 of 119) of the potentially overdiagnosed cases of lung cancer originated from the initial screening. In other words, overdiagnosis may be more infrequent during subsequent screening rounds. This argument may justify repeated lung cancer screening efforts using LDCT. We are eagerly anticipating the final report by the ITALUNG researchers so that we can analyze the effect of overdiagnosis in lung cancer screening using LDCT.

Disclosure: The authors declare no conflict of interest.

Address for correspondence: Yuichi Takiguchi, MD, PhD, Department of Medical Oncology, Graduate School of Medicine, Chiba University, 1-8-1, Inohana, Chuo-ku, Chiba, 260–8670 Japan. E-mail: takiguchi@faculty.chiba-u.jp

ISSN: 1556-0864/13/0811-0e101

Yuichi Takiguchi, MD, PhD
Ikuo Sekine, MD, PhD
Shunichiro Iwasawa, MD, PhD
Department of Medical Oncology
Graduate School of Medicine
Chiba University
Chiba, Japan

REFERENCES

1. Lopes Pegna A, Picozzi G, Falaschi F, et al.; ITALUNG Study Research Group. Four-year results of low-dose CT screening and nodule management in the ITALUNG trial. *J Thorac Oncol* 2013;8:866–875.
2. Aberle DR, Adams AM, Berg CD, et al. Reduced lung-cancer mortality with low-dose computed tomographic screening. *New Engl J Med* 2011; 365: 395–409.
3. Church TR, Black WC, Aberle DR, et al. Results of initial low-dose computed tomographic screening for lung cancer. *New Engl J Med* 2013; 368: 1980–1991.

In Response:

We thank Dr. Takiguchi and colleagues for their comments on our article reporting the final results concerning cancer detection and lesion management in the arm undergoing low-dose computed tomography (LDCT) screening of the ITALUNG trial.[1] To explain the higher detection rate of lung cancers at baseline LDCT screening round as compared with the three subsequent annual repeat LDCT screening rounds observed in our study and in the National Lung Screening Trial (NLST) in the United States,[2] they hypothesized that indolent cancers tend to accumulate preferentially without presenting symptoms at baseline, leading to a higher rate of overdiagnosis, than during subsequent screening rounds, a phenomenon known to occur in breast cancer screening with mammography.[3]

Overdiagnosis is defined as the possibility that screening determines detection of a relevant number of cancers that would not have otherwise become clinically apparent in the subject's lifetime.[4] Two components of overdiagnosis bias in lung cancer screening are recognized.[5] First, the detection of slowly growing lung cancers with low probability of malignant progression[6] and, second, the detection of cancers in subjects who would have had low probability of dying of a given type of cancer in their lifetime because of competing causes of death. The latter component is particularly relevant in elderly heavy smokers and former smokers in consideration of the frequency of cardiovascular disease. Theoretically, at least three approaches can be adopted to study overdiagnosis in lung cancer screening: the epidemiological one (see below), the imaging-based one, which entails measurement of tumour doubling time reflecting local growth capability,[7] and the pathological one, which is based on the characterization of structural and biomarkers features of tumor aggressiveness.

In general, overdiagnosis can be estimated in randomized clinical trials (RCTs) by comparing the cumulative cancer incidence in the screened versus the unscreened groups at the end of a long follow-up period, typically at least 5–10 years, after conclusion of study period and in absence of any screening in the control arm.[8] In the absence of overdiagnosis the ratio of cumulative cancer incidence between screened and unscreened group should be 1, whereas any excess of lung cancer cases in the screened group can be considered as expression of overdiagnosis. Such an estimate of overdiagnosis is not yet possible in the NLST because of the short follow-up after the end of the study. Moreover, we would like to underline that subjects in the control group of NLST received chest radiograph annually[2] and the possible overdiagnosis bias related to chest radiograph ray screening is unknown. We are confident that results from RCTs should enable in the future a better assessment of overdiagnosis, which is an important potential harm of lung cancer screening with LDCT. In particular, we are of the opinion that a quantitative estimate of overdiagnosis can be expected, in due time, from European RCTs, like Nederalnds Luevens Longkanker Screeningonderzoek (NELSON)[9] and ITALUNG[1] in which no screening test has been offered to subjects randomized to the control group.

For the present, in our opinion, the higher incidence at baseline as compared with subsequent screening rounds in ITALUNG[1] and NLST[2] trials can be explained by lead time and should not considered per se a proof of overdiagnosis.[5]

Mario Mascalchi, MD, PhD
Quantitative and Functional Radiology, "Mario Serio"
Department of Experimental and Clinical Biomedical Sciences
University of Florence
Florence, Italy

Andrea Lopes-Pegna, MD
Pneumonology Unit
Careggi University Hospital
Florence, Italy

Eugenio Paci, MD
Epidemiology Section
ISPO
Florence, Italy

REFERENCES

1. Lopes Pegna A, Picozzi G, Falaschi F, et al.; ITALUNG Study Research Group. Four-year results of low-dose CT screening and nodule management in the ITALUNG trial. *J Thorac Oncol* 2013;8:866–875.
2. Church TR, Black WC, Aberle DR, et al. Results of initial low-dose computed tomographic screening for lung cancer. *New Engl J Med* 2013;368:1980–1991.
3. Yen AM, Duffy SW, Chen TH, et al. Long-term incidence of breast cancer by trial arm in one county of the Swedish Two-County Trial of mammographic screening. *Cancer* 2012;118:5728–5732.
4. Paci E, Duffy S. Overdiagnosis and overtreatment of breast cancer: overdiagnosis and overtreatment in service screening. *Breast Cancer Res* 2005;7:266–270.
5. Paci E. Observational, one-arm studies and randomized population-based trials for evaluation of the efficacy of lung cancer screening. *J Thorac Oncol* 2007;2(5 Suppl):S45–S46.
6. Bach PB. Is our natural-history model of lung cancer wrong? *Lancet Oncol* 2008;9:693–697.
7. Henschke CI, Yankelevitz DF, Yip R, et al.; Writing Committee for the I-ELCAP Investigators. Lung cancers diagnosed at annual CT screening: volume doubling times. *Radiology* 2012;263:578–583.
8. Biescheuvel C, Barrat A, Howard K, et al. Effects of study methods and biases on estimates of invasive breast cancer overdetection with mammographic screening: a systematic review. *Lancet Oncol* 2007;8:1129–1138.

Disclosure: The authors declare no conflict of interest.

Address for correspondence: Professor Mario Mascalchi at "Mario Serio," Department of Experimental and Clinical Biomedical Sciences, University of Florence, Viale Pieraccini 6, 50100 Florence, Italy. E-mail: m.mascalchi@dfc.unifi.it

ISSN: 1556-0864/13/0811-0e102

Hindawi Publishing Corporation
Case Reports in Ophthalmological Medicine
Volume 2013, Article ID 213124, 3 pages
http://dx.doi.org/10.1155/2013/213124

Case Report

Choroidal Metastasis of Non-Small Cell Lung Cancer That Responded to Gefitinib

Iwao Shimomura,[1] Yuji Tada,[1] Gen Miura,[2] Toshio Suzuki,[1] Takuma Matsumura,[1] Kenji Tsushima,[1] Jiro Terada,[1] Ryota Kurimoto,[3] Emiko Sakaida,[3] Ikuo Sekine,[3] Yuichi Takiguchi,[3] Shuichi Yamamoto,[2] and Koichiro Tatsumi[1]

[1] *Department of Respirology, Graduate School of Medicine, Chiba University, 1-8-1 Inohana Chuo-ku, Chiba 260-8677, Japan*
[2] *Department of Ophthalmology and Visual Science, Graduate School of Medicine, Chiba University, 1-8-1 Inohana Chuo-ku, Chiba 260-8677, Japan*
[3] *Department of Medical Oncology, Graduate School of Medicine, Chiba University, 1-8-1 Inohana Chuo-ku, Chiba 260-8677, Japan*

Correspondence should be addressed to Yuji Tada; ytada25@yahoo.co.jp

Received 28 June 2013; Accepted 14 August 2013

Academic Editors: A. A. Bialasiewicz, H. Y. Chen, N. Fuse, and M. Rosner

A 52-year-old Japanese woman presented with optical symptoms, including left-sided myodesopsia, blurred vision, narrowed visual field, and diminished visual acuity. Ocular evaluation revealed a metastatic tumor in the choroid. Further examinations identified pulmonary adenocarcinoma as the primary tumor. Because an epidermal growth factor receptor gene (*EGFR*) mutation was detected in a biopsy specimen, gefitinib treatment was initiated. Dramatic responses were obtained in the primary tumor and metastatic foci. Optical symptoms improved and remained stable for 5 months during the treatment, until relapse. This report demonstrates that gefitinib is effective for choroidal metastasis of pulmonary adenocarcinoma harboring an *EGFR* mutation.

1. Introduction

The choroid is the most common ocular site for metastasis due to its abundant blood supply. Only one-third of patients with choroidal metastasis have the primary tumor site identified at the time of diagnosis [1]. The two major primary sites are the breast and lung, and lung cancer accounts for approximately 30% of choroidal metastasis [2]. Visual symptoms may be the first manifestation of systemic metastases. Visual impairment includes myodesopsia, blurred vision, narrowed visual field, and lower visual acuity. These symptoms are caused not only by the mass effect of the tumor, but also by increased subretinal fluid, retinal edema, and retinal detachment. Persistent retinal detachment ultimately results in irreversible visual loss that greatly reduces the patient's quality of life (QOL).

Because two-third-of-patients with choroidal metastasis of lung cancer are benefitted by any treatment [3], early recognition and therapy are important to maximize a patient's QOL. In general, systemic chemotherapy alone is effective if the original tumor is susceptible to the cytotoxic agents. Recent progress in molecular targeted drugs has demonstrated favorable outcome for ocular tumors due to their prompt and high response rate [1, 2]. Epidermal growth factor receptor tyrosine kinase inhibitor (EGFR-TKi) is also expected to be a promising treatment for ocular metastasis of non-small cell lung cancer (NSCLC) harboring an *EGFR* mutation, although little information has been provided.

2. Case Report

A 52-year-old Japanese woman, a current smoker, presented with optical symptoms, including left-sided myodesopsia, blurred vision, narrowed visual field, and diminished visual acuity. Because these symptoms gradually became worse, she was referred to the ophthalmologist a month after symptom onset. Ocular evaluation by fundoscopy and optical coherence tomography (OCT) revealed a solitary metastatic

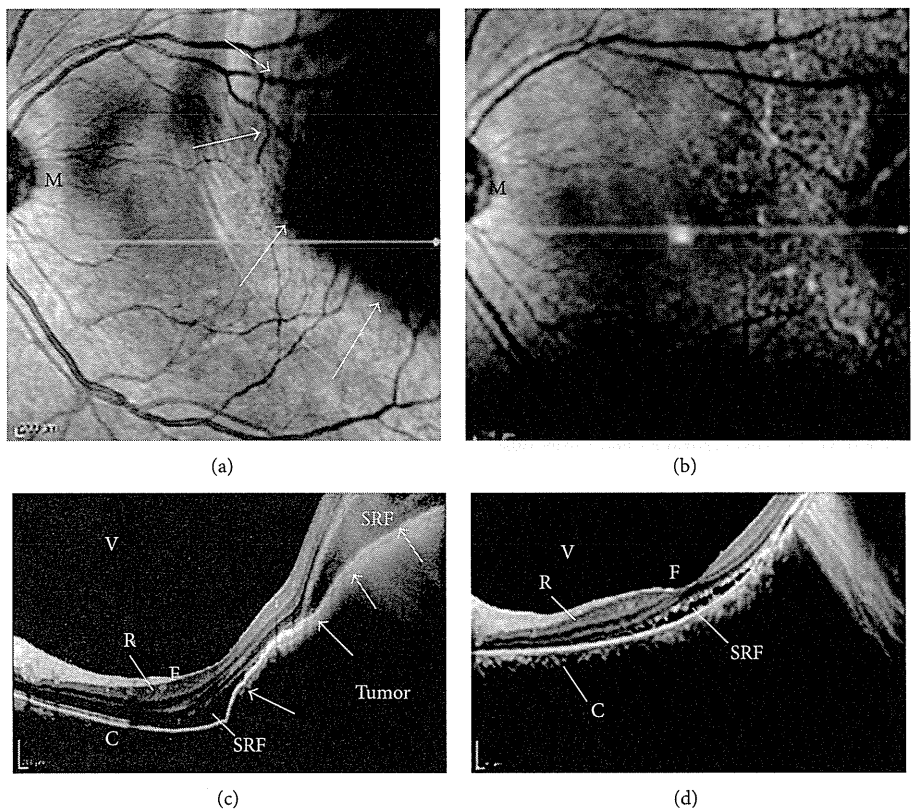

FIGURE 1: (a) Photograph of fundoscopy in the involved eye (left-side) before gefitinib treatment. A large elevated lesion in the superotemporal quadrant was found (arrows) with exudation. The patient's best corrected visual acuity in the left eye was 20/200 before treatment. (M: macula). (b) The elevated lesion disappeared a month after the onset of gefitinib treatment. Her best corrected visual acuity in the left eye improved to 20/100 after treatment. (c) Optical coherence tomography (OCT) before treatment corresponding to (a). A dome-shaped large mass with high reflectivity occupied the choroid, pushing the retina into the vitreous-cavity side (arrows). Accumulation of the subretinal fluid was also observed. (C: choroid, F: fovea centralis, R: retina, SRF: subretinal fluid, V: vitreous body). (d) Complete flattening of the tumor and decreased subretinal fluid were observed, demonstrating a dramatic response to gefitinib.

choroid tumor in her left eye (Figures 1(a) and 1(c)). Her best corrected visual acuity was 20/16 in the right eye and 20/200 in the left eye. For the ocular lesion, systemic chemotherapy was recommended by the ophthalmologist because the tumor size was beyond the scope of local treatment such as external-beam irradiation.

Subsequently, a chest computed tomography (CT) scan and transbronchial biopsy (TBB) were performed to diagnose adenocarcinoma of the lung. She had malignant pleural effusion and multiple metastatic foci in bones that were asymptomatic (Figure 2(a)). The stage of her disease was determined as IV (T4N3M1b). Genetic testing of the TBB specimens identified an exon 19 deletion mutation (delE746-A750) of *EGFR*. This mutation predicts beneficial response to EGFR-TKi. She was administered oral gefitinib (250 mg daily) as the first-line treatment, which yielded dramatic responses both in the primary site and metastatic lesions within a month (Figure 2(b)). Fundoscopy (Figures 1(a) and 1(b)) and OCT (Figures 1(c) and 1(d)) revealed the almost complete disappearance of the choroidal tumor and reduction of the subretinal fluid a month after gefitinib initiation. Although the improvement of visual acuity was slight (from 20/200 to 20/100 in the left eye), myodesopsia and blurred vision dramatically improved by 3 weeks after the treatment and remained stable during the first-line therapy. Unfortunately, gefitinib was discontinued due to disease progression, with new brain metastases becoming apparent. The subsequent chemotherapy consisted of cisplatin and pemetrexed; however, these failed to improve the visual symptoms and elicited no tumor shrinkage. However, she was satisfied with the improved vision that lasted for approximately 5 months during the gefitinib treatment course, until relapse.

3. Discussion

In this paper, we showed the effectiveness of gefitinib for choroidal metastasis of NSCLC as the first-line treatment. To our knowledge, only three reports have previously used EGFR-TKi to treat choroidal metastasis of NSCLC [3–5]. However, two of these reports lack detailed information regarding the *EGFR* mutation, and one used erlotinib in combination with intravitreal bevacizumab. Because patients

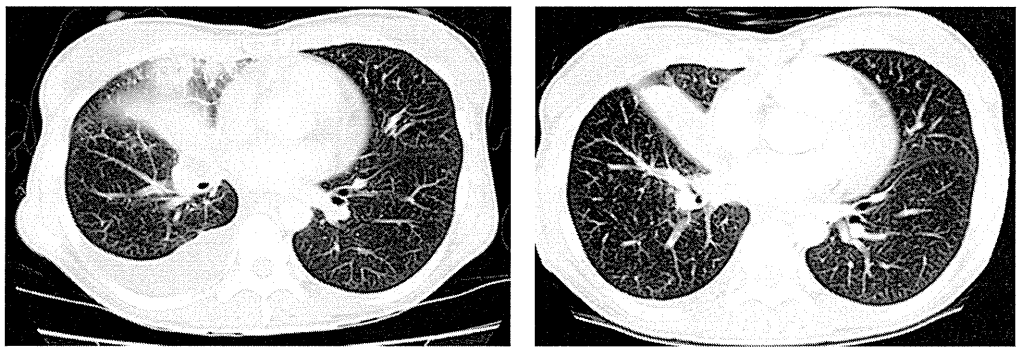

(a) (b)

FIGURE 2: Chest computed tomography (CT) scan before treatment (a) and a month after gefitinib initiation (b). Size reduction of the primary tumor and disappearance of right-sided pleural effusion were observed.

with normal EGFR gain no benefit from administering gefitinib [6], it is crucial to demonstrate the *EGFR* mutation status before choosing this treatment.

The choroid is external to the blood-retinal barrier, and systemic medication freely diffuses into the choroid via the fenestrated endothelium of choroid capillaries [5]. This is different from retinal tumors, which are protected from systemic drug exposure by the blood-retinal barrier. Systemic chemotherapy alone is thus effective for choroid metastases if the primary tumor is susceptible to anticancer agents. In NSCLC, however, systemic chemotherapy with cytotoxic drugs has drawbacks such as the time delay to the first response and limited drug efficacy. One of the merits of first-line EGFR-TKI is the prompt and dramatic response for patients with an *EGFR* mutation. We demonstrated that our patient expressed an exon 19 deletion mutation of *EGFR* in the primary tumor site and required a rapid response to avoid irreversible visual symptoms; therefore, we chose gefitinib as the first-line treatment. Indeed, almost complete remission of the choroidal lesion was achieved within a month.

For patients with NSCLC harboring EGFR mutations, complete use of EGFR-TKi is the key to success in treatment [6]. Recent studies have demonstrated that, compared with platinum doublets, first-line gefitinib prolonged progression-free survival while preserving a favorable QOL [7]. In the present case, blurred vision and narrowed visual field were promptly improved by gefitinib. Because visual impairment is a key factor that has an impact on a patient's QOL, we believe that EGFR-TKi should be initiated early in the treatment course [8].

Unfortunately, gefitinib was delivered for only 5 months before the disease progressed via new brain metastasis. How much benefit do patients gain by continuing EGFR-TKi beyond the disease progression is a matter that warrants further discussion.

In conclusion, we have shown the effective use of EGFR-TKis for choroidal metastasis of NSCLC with an *EGFR* mutation. To prevent or at least delay irreversible visual loss, EGFR-TKi should be initiated earlier and should be continued as long as possible during treatment.

Conflict of Interests

The authors report no conflict of interests.

References

[1] E. Munzone, F. Nolè, G. Sanna, and A. Goldhirsch, "Response of bilateral choroidal metastases of breast cancer to therapy with trastuzumab," *Breast*, vol. 14, no. 5, pp. 380–383, 2005.

[2] I. C. Kuo, J. A. Haller, R. Maffrand, R. H. Sambuelli, and V. E. Reviglio, "Regression of a subfoveal choroidal metastasis of colorectal carcinoma after intravitreous bevacizumab treatment," *Archives of Ophthalmology*, vol. 126, no. 9, pp. 1311–1313, 2008.

[3] M. Inoue, Y. Watanabe, S. Yamane et al., "Choroidal metastasis with adenocarcinoma of the lung treated with gefitinib," *European Journal of Ophthalmology*, vol. 20, no. 5, pp. 963–965, 2010.

[4] S.-W. Kim, M. J. Kim, K. Huh, and J. Oh, "Complete regression of choroidal metastasis secondary to non-small-cell lung cancer with intravitreal bevacizumab and oral erlotinib combination therapy," *Ophthalmologica*, vol. 223, no. 6, pp. 411–413, 2009.

[5] C. J. Chen, A. N. McCoy, J. Brahmer, and J. T. Handa, "Emerging treatments for choroidal metastases," *Survey of Ophthalmology*, vol. 56, no. 6, pp. 511–521, 2011.

[6] T. S. Mok, Y.-L. Wu, S. Thongprasert et al., "Gefitinib or carboplatin-paclitaxel in pulmonary adenocarcinoma," *The New England Journal of Medicine*, vol. 361, no. 10, pp. 947–957, 2009.

[7] S. C. Verduyn, B. Biesma, F. M. Schramel et al., "Estimating quality adjusted progression free survival of first-line treatments for EGFR mutation positive non small cell lung cancer patients in The Netherlands," *Health Qual Life Outcomes*, vol. 10, p. 108, 2012.

[8] C. M. Patino, R. Varma, S. P. Azen, D. V. Conti, M. B. Nichol, and R. McKean-Cowdin, "The impact of change in visual field on health-related quality of life: the Los Angeles Latino eye study," *Ophthalmology*, vol. 118, no. 7, pp. 1310–1317, 2011.

FULL PAPER

BJC

British Journal of Cancer (2013) 108, 1817–1821 | doi: 10.1038/bjc.2013.175

Keywords: oral squamous cell carcinoma (OSCC); microRNA; miR-125b; intercellular adhesion molecule 2 (ICAM2); radioresistance

MicroRNA-125b regulates proliferation and radioresistance of oral squamous cell carcinoma

M Shiiba*[,1,2], K Shinozuka[1], K Saito[3], K Fushimi[1], A Kasamatsu[1], K Ogawara[1], K Uzawa[1], H Ito[4], Y Takiguchi[2] and H Tanzawa[1]

[1]*Department of Clinical Molecular Biology, Graduate School of Medicine, Chiba University, 1-8-1 Inohana, Chuo-ku, Chiba 260-8670, Japan;* [2]*Department of Medical Oncology, Graduate School of Medicine, Chiba University, 1-8-1 Inohana, Chuo-ku, Chiba 260-8670, Japan;* [3]*Department of Molecular Virology, Graduate School of Medicine, Chiba University, 1-8-1 Inohana, Chuo-ku, Chiba 260-8670, Japan and* [4]*Department of Radiology, Graduate School of Medicine, Chiba University, 1-8-1 Inohana, Chuo-ku, Chiba 260-8670, Japan*

Background: MicroRNAs (miRNAs) are involved in essential biological activities, and have been reported to exhibit differential expression profiles in various cancers. Our previous study demonstrated that *intercellular adhesion molecule-2* (*ICAM2*) inhibition induces radiosensitisation in oral squamous cell carcinoma (OSCC) cells. Thus, we hypothesised that certain miRNAs play crucial roles in radioresistance in OSCC by regulating *ICAM2* expression.

Methods: Because predicted target gene analyses revealed that microRNA-125b (miR-125b) potentially regulates *ICAM2* mRNA expression, we examined the association between miR-125b and radioresistance. The expression of miR-125b was investigated by real-time quantitative reverse transcriptase–PCR. For a functional analysis, miR-125b was transfected to OSCC-derived cells.

Results: A downregulated expression of miR-125b was found in OSCC-derived cell lines and OSCC samples. The miR-125b-transfected cells showed a decreased proliferation rate, enhanced radiosensitivity to X-ray irradiation and diminished *ICAM2* mRNA expression. Moreover, miR-125b expression correlated with OSCC tumour staging and survival.

Conclusion: These findings suggested that the downregulated miR-125b expression was associated with proliferation and radioresistance mechanisms, probably through ICAM2 signalling. Thus, controlling the expression or activity of miR-125b might contribute to suppressing proliferation and overcoming radioresistance in OSCC.

MicroRNAs (miRNAs) are involved in essential biological activities (Harfe, 2005; Carleton *et al*, 2007). Recent studies have revealed differential expression of miRNAs in various cancers, including oral cancer, suggesting that certain miRNAs play roles in tumourigenesis (Garzon *et al*, 2009; Wu *et al*, 2011). In addition, previous studies have revealed that some miRNAs are closely associated with clinical outcomes (Schetter *et al*, 2008). Moreover, miRNA expression may predict the efficacy of therapies, including radiotherapy (Niemoeller *et al*, 2011). In fact, miRNAs have been shown to modulate the radiosensitivity of primary human dermal microvascular endothelial cells (Wagner-Ecker *et al*, 2010), lung cancer cells (Weidhaas *et al*, 2007) and breast cancer cells (Kato *et al*, 2009). However, irradiation-induced alterations in miRNA profiles have not been analysed in oral squamous cell carcinoma (OSCC). Thus, this study aimed to identify miRNAs associated with radioresistance in OSCC and reveal their biological function and clinical significance.

*Correspondence: Dr M Shiiba; E-mail: m.shiiba@faculty.chiba-u.jp

Revised 4 March 2013; accepted 25 March 2013; published online 18 April 2013

MATERIALS AND METHODS

Analysis of predicted target genes. To identify crucial miRNAs for *intercellular adhesion molecule-2* (*ICAM2*) expression, we examined miRNAs that had binding sites like *ICAM2* and had been reported to be related to human cancer, especially proliferation, radioresistance and chemoresistance, with publicly available algorithms (TargetScan (http://www.targetscan.org/), EMBL-EBI (http://www.ebi.ac.uk/) or microRNA.org (http://www.microrna.org/microrna/)).

Cell lines and tissue specimens. The OSCC-derived cell lines used were HSC-2, HSC-3, HSC-4, SCC4, HO-1-N-1 and Ca9-22 (Human Science Research Resources Bank, Osaka, Japan). Five independent human normal oral keratinocyte (HNOK) cell lines were cultured and maintained in defined keratinocyte-serum-free medium (Life Technologies Corporation, Grand Island, NY, USA) (Shiiba *et al*, 2010). Tissue samples from 50 unrelated Japanese patients with primary OSCC who were treated at Chiba University Hospital (Supplementary Table 1) were collected after obtaining informed consents under a protocol that was approved by the Chiba University institutional review board.

RNA extraction and reverse transcription. Total RNA was extracted with TRIzol Reagent (Life Technologies Corporation) according to the manufacturer's instructions. Complementary DNA (cDNA) was synthesised from total RNA using Ready-To-Go You-Prime First-Strand Beads (GE Healthcare, Little Chalfont, UK), an oligo(dT) primer (Sigma-Aldrich Co. LLC, St Louis, MO, USA) for *ICAM2* and the NCode VILO miRNA cDNA Synthesis Kit (Life Technologies Corporation) for miRNA, according to the manufacturers' protocols.

Real-time quantitative reverse transcriptase–PCR (qRT–PCR) analysis. Real-time qRT–PCR was performed to validate miRNA and mRNA expression with the NCode EXPRESS SYBR GreenER microRNA qRT–PCR Kit (Life Technologies Corporation) for miRNA and a LightCycler FastStart DNA Master SYBR Green 1 Kit (Roche Diagnostics GmbH, Mannheim, Germany) for mRNA. Normalised expression was calculated with 18S ribosomal RNA for miRNA and glyceraldehyde-3-phosphate dehydrogenase for mRNA. Transcript amount was estimated from standard curves and normalised. The nucleotide sequences of the specific primers for miRNAs and *ICAM2* are shown in Supplementary Table 2.

Transfection with miR-125b. The HSC-2 and HSC-3 cells (2×10^5) were transfected with mirVana miRNA mimic (microRNA-125b) and mirVana miRNA Mimic Negative Control #1 (Life Technologies Corporation) at a final concentration of 50 nM. The cells were transfected with miRNA duplexes with Lipofectamine 2000 reagent (Life Technologies Corporation) by following the manufacturer's protocol. The pmax-green fluorescent protein (GFP) plasmid (Lonza Group Ltd, Basel, Switzerland) was co-transfected simultaneously, and the transfection efficiency was determined by analysing GFP-expressing cells with flow cytometry.

Construction of reporter plasmids and luciferase reporter assays. The full-length 3′-untranslated region (UTR) of *ICAM2* containing putative miR-125b-binding sites was subcloned into a pmirGLO Dual-Luciferase miRNA Target Expression Vector (Promega Corporation, Madison, WI, USA) located 3′ to the firefly luciferase translational stop codon. A mutant 3′-UTR of *ICAM2* with a mutated sequence (5′-...AACTCAGTGTGACT-C***ATCGATC***TTGAGGTCC...-3′) in the complementary site for the miR-125b seed region was generated with fusion PCR (mutated sequence is expressed as italic and underlined). For the luciferase

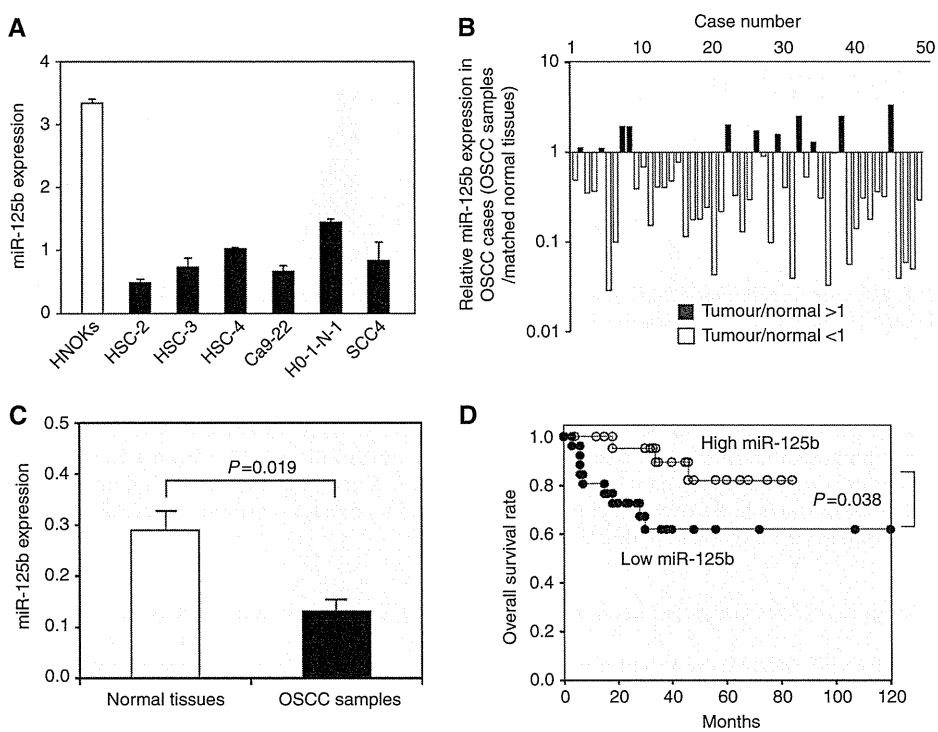

Figure 1. Expression profiles of miR-125b in oral squamous cell carcinoma (OSCC)-derived cell lines and OSCC samples. The quantification of miR-125b expression levels in OSCC-derived cell lines (**A**) and OSCC samples (**B**) was performed by real-time qRT–PCR analyses. The data are expressed as means ± s.d. Significantly lower miR-125b expression levels were detected in primary OSCCs compared with matched normal tissues ($P = 0.019$, Student's *t*-test) (**C**). The data are expressed as means ± s.d. The overall survival rate was investigated by Kaplan–Meier analysis (**D**). Lower miR-125b expression levels were significantly associated with poor outcome in patients with OSCC. The log-rank test revealed significant *P*-values ($P = 0.038$).

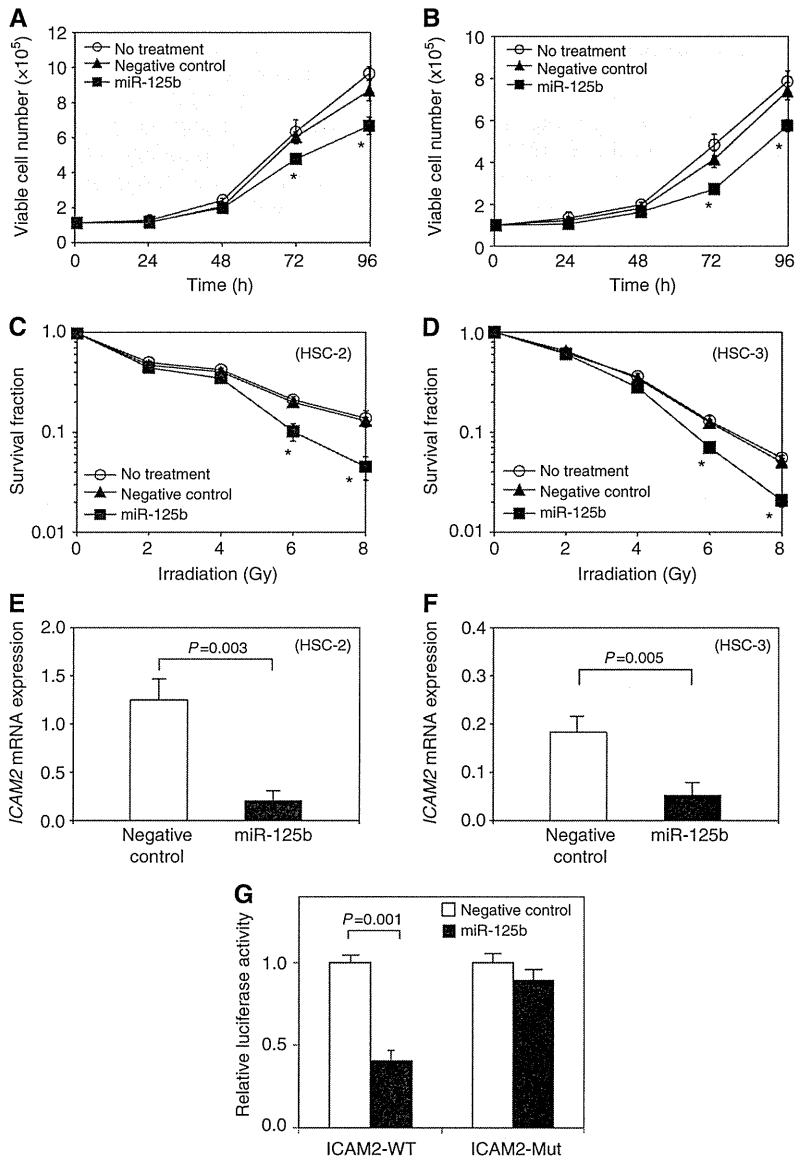

Figure 2. Effect of miR-125b overexpression on OSCC-derived cell lines. A cellular proliferation assay was performed to investigate the effects of the overexpression of miR-125b on the OSCC-derived cell lines HSC-2 (**A**) and HSC-3 (**B**). *Significant differences between transfectants and negative controls (NCs; $P<0.05$, Student's *t*-test). The data are expressed as means ± s.d. Cell survival after irradiation was examined with a clonogenic survival assay (**C** and **D**). After exposure to 2, 4, 6 and 8 Gy of X-ray irradiation, cells were seeded and cultured. The significance of the differences between transfectant and NC cells is indicated with asterisks (*) ($P<0.05$, Student's *t*-test). The data are expressed as means ± s.d. The *ICAM2* mRNA expression in miR-125b-transfected cells and NC cells in HSC-2 (**E**) and HSC-3 (**F**) is shown. The expression levels of *ICAM2* mRNA were decreased after the introduction of miR-125b to both cell lines ($P<0.01$, Student's *t*-test). The data are expressed as means ± s.d. The luciferase activity of the reporter gene containing the wild-type 3′-UTR of the *ICAM2* gene (*ICAM2*-WT) or the mutated 3′-UTR of the *ICAM2* gene (*ICAM2*-Mut) was determined (**G**). The data are expressed as means ± s.d. Relative luciferase activity was significantly suppressed in the cells with *ICAM2*-WT when miR-125b was co-transfected ($P=0.001$, Student's *t*-test).

reporter assay, HSC-2 cells (5×10^4) were placed in 24-well plates and co-transfected with 0.2 μg of pmirGLO-3′-UTR-WT (*ICAM2*-WT) or pmirGLO-3′-UTR-MUT (*ICAM2*-Mut) and miR-125b or negative control with Lipofectamine 2000 (Life Technologies Corporation). Assays were performed 24 h after transfection with the Dual-Luciferase Reporter Assay System (Promega Corporation). Transfections were done three times in independent experiments.

Cell proliferation assay. Transfectant and parental cells were seeded in 12-well plates (1×10^4 viable cells per well). Cells were harvested 1, 2, 3 and 4 days later, and the cells were trypsinised and counted with a haemocytometer in triplicate.

X-ray irradiation and clonogenic survival assay. Transfectant and parental cells were irradiated with four single-radiation doses (2, 4, 6 and 8 Gy) with X-ray-irradiation equipment (MBR-1520 R-3; Hitachi, Tokyo, Japan) at a source-to-target distance of 55 cm when the cells reached 70–80% confluence (Higo *et al*, 2005; Ishigami *et al*, 2008). The colonies were stained with crystal violet (Sigma-Aldrich Co. LLC), and colonies of $\geqslant 50$ cells were counted (Ishigami *et al*, 2008). Each experiment was repeated at least three times.

Statistical analysis. Clinicopathological profiles were assessed by χ^2 tests and Fisher's exact tests. Overall survival rate was

Table 1. Correlation between miR-125b expression and clinicopathological profiles

		MicroRNA-125b expression		
Clinicopathological profiles	**n**	**Low (<median)**	**High (>median)**	***P*-value**
Tumour size (T)				
T1	5	1 (20%)	4 (80%)	$P=0.086$[a]
T2	14	5 (36%)	9 (64%)	
T3	10	8 (80%)	2 (20%)	
T4	21	11 (53%)	10 (47%)	
T1+T2	19	6 (32%)	13 (68%)	$P=0.079$[b]
T3+T4	31	19 (61%)	12(39%)	
Regional lymph node metastasis (*N*)				
Negative	33	16 (48%)	17 (52%)	$P=0.765$[a]
Positive	17	9 (53%)	8 (47%)	
Stage classification				
I	5	1 (20%)	4 (80%)	$P=0.100$[a]
II	6	1 (17%)	5 (83%)	
III	7	5 (71%)	2 (29%)	
IV	32	18 (56%)	14 (44%)	
I+II	11	2 (18%)	9 (82%)	$P=0.037$[b]
III+V	39	23 (59%)	16 (41%)	
Differentiation				
Well	28	13 (46%)	15 (54%)	$P=0.776$[b]
Moderate + poor	22	12 (55%)	10 (45%)	

[a]The χ^2 test.
[b]Fisher's exact test.

investigated by Kaplan–Meier analyses, and the difference was analysed with log-rank tests. Student's *t*-tests were used for other analyses. All tests were two sided. $P<0.05$ was considered significant.

RESULTS

Analysis of the predicted target gene. We initially performed predicted target gene analyses of *ICAM2* mRNA with publicly available algorithms to find miRNA that potentially regulated *ICAM2* expression. The databases showed that miR-125b had complementary sequences for *ICAM2* mRNA, suggesting that miR-125b could directly regulate *ICAM2* activity through imperfect base pairing with the *ICAM2* mRNA 3′-UTR (Supplementary Figure 1A–C). Altered miR-125b expression has been reported in various human cancers, and miR-125b-induced cell cycle arrest has been reported for several cancers (Guan *et al*, 2011; Huang *et al*, 2011; Zhang *et al*, 2011). We hypothesised that miR-125b plays a role in OSCC by regulating *ICAM2* expression. Thus, miR-125b was analysed further.

The miR-125b levels in OSCC-derived cell lines and OSCC samples. The expression of miR-125b was less than twice that of HNOK cells in all cell lines (Figure 1A). Lower expression levels were observed in 39 of 50 (78%) OSCC samples compared with matched normal tissues (Figure 1B). The median miR-125b expression level was 0.280 and 0.132 in normal tissues and OSCC samples, respectively (Figure 1C), which was significant ($P=0.019$; Student's *t*-test).

The relationship between clinical factors and miR-125b expression was evaluated (Table 1). The expression of miR-125b was significantly lower in advanced stages (III + IV) than in early stages (I + II) ($P=0.037$).

Prognostic significance of miR-125b expression in OSCC. Tumours with significant miR-125b downregulation (median <0.34) were considered low miR-125b ($n=25$). Survival curves for miR-125b expression are shown in Figure 1D. Kaplan–Meier analyses indicated that miR-125b expression was significantly associated with overall survival ($P=0.038$; Figure 1D), suggesting that decreased miR-125b expression in patients with OSCCs was significantly associated with poor prognoses.

Effects of miR-125b overexpression on cellular proliferation and radiosensitivity. After validating miR-125b overexpression (Supplementary Figure 2A and B) with appropriate transfection efficiency, miR-125b-transfected cells were subjected to functional assays. The proliferation rate was significantly lower in miR-125b-transfected HSC-2 and HSC-3 cells after 72 and 96 h compared with negative controls (Figures 2A and B). In HSC-2 and HSC-3 cells, the survival rates were significantly decreased in 6-Gy-irradiated and 8-Gy-irradiated miR-125b transfectants compared with negative controls (Figures 2C and D).

The miR-125b overexpression suppressed ICAM2 expression in OSCC-derived cell lines. We examined whether altered radiosensitivity was associated with the ICAM2-related signalling pathway. The expression of *ICAM2* was downregulated in miR-125b-transfected OSCC cells (Figure 2E and F).

MiR-125b targets ICAM2. The relative luciferase activity of the reporter gene containing wild-type *ICAM2* 3′-UTR was

significantly suppressed when miR-125b was co-transfected. However, decreased luciferase activity was not observed in cells with the reporter gene containing mutated *ICAM2* 3′-UTR (Figure 2G). This suggested that the *ICAM2* 3′-UTR was a miR-125b target and that miR-125b suppressed *ICAM2* expression through binding.

DISCUSSION

We have previously identified genes, including *ICAM2*, that play important roles in OSCC radioresistance (HSC-2 and HSC-3) (Ishigami *et al*, 2007, 2008). The *ICAM2* has been suggested to facilitate an apoptotic-blocking survival signal by activating the PI3K/AKT pathway (Perez *et al*, 2002). Another study has reported that *ICAM2* expression deficiencies result in impaired angiogenesis *in vitro* and *in vivo*, defective *in vitro* migration and increased apoptosis (Huang *et al*, 2005). The downregulation of *ICAM2* siRNA enhanced OSCC radiosensitivity and increased apoptosis through AKT phosphorylation and caspase-3 activation (Ishigami *et al*, 2008). Moreover, *ICAM2* overexpression induced greater OSCC resistance to X-ray irradiation (Ishigami *et al*, 2007).

In this study, decreased *ICAM2* expression was observed in both miR-125b-transfected HSC-2 and miR-125b-transfected HSC-3 cells; moreover, radiosensitivity towards X-ray irradiation was enhanced in miR-125b-transfected HSC-2 and HSC-3 cells. Luciferase reporter assays showed that the *ICAM2* 3′-UTR was a miR-125b target. Therefore, the data strongly suggest that miR-125b is associated with radiation response through regulating *ICAM2* expression in OSCC.

The importance of miR-125b as an anticancer agent was demonstrated by the impact of its expression on cell proliferation. We showed that OSSC-derived cells proliferated less rapidly when miR-125b expression was increased by transfection, suggesting that miR-125b could regulate cell proliferation. This finding may be associated with cell cycle regulation as miR-125b-induced cell cycle arrest has been reported for several cancers (Guan *et al*, 2011; Huang *et al*, 2011; Zhang *et al*, 2011).

In conclusion, controlling miR-125b expression or activity could contribute to suppressing cell proliferation and overcoming radioresistance in OSCC, which could be useful in developing a cure for OSCC. Moreover, miR-125b was significantly correlated with survival and radiotherapy response in OSCC and could be used as a prognostic marker.

REFERENCES

Carleton M, Cleary MA, Linsley PS (2007) MicroRNAs and cell cycle regulation. *Cell Cycle* **6**: 2127–2132.

Garzon R, Calin GA, Croce CM (2009) MicroRNAs in cancer. *Annu Rev Med* **60**: 167–179.

Guan Y, Yao H, Zheng Z, Qiu G, Sun K (2011) MiR-125b targets BCL3 and suppresses ovarian cancer proliferation. *Int J Cancer* **128**: 2274–2283.

Harfe BD (2005) MicroRNAs in vertebrate development. *Curr Opin Genet Dev* **15**: 410–415.

Higo M, Uzawa K, Kouzu Y, Bukawa H, Nimura Y, Seki N, Tanzawa H (2005) Identification of candidate radioresistant genes in human squamous cell carcinoma cells through gene expression analysis using DNA microarrays. *Oncol Rep* **14**: 1293–1298.

Huang L, Luo J, Cai Q, Pan Q, Zeng H, Guo Z, Dong W, Huang J, Lin T (2011) MicroRNA-125b suppresses the development of bladder cancer by targeting E2F3. *Int J Cancer* **128**: 1758–1769.

Huang MT, Mason JC, Birdsey GM, Amsellem V, Gerwin N, Haskard DO, Ridley AJ, Randi AM (2005) Endothelial intercellular adhesion molecule (ICAM)-2 regulates angiogenesis. *Blood* **106**: 1636–1643.

Ishigami T, Uzawa K, Fushimi K, Saito K, Kato Y, Nakashima D, Higo M, Kouzu Y, Bukawa H, Kawata T, Ito H, Tanzawa H (2008) Inhibition of ICAM2 induces radiosensitization in oral squamous cell carcinoma cells. *Br J Cancer* **98**: 1357–1365.

Ishigami T, Uzawa K, Higo M, Nomura H, Saito K, Kato Y, Nakashima D, Shiiba M, Bukawa H, Yokoe H, Kawata T, Ito H, Tanzawa H (2007) Genes and molecular pathways related to radioresistance of oral squamous cell carcinoma cells. *Int J Cancer* **120**: 2262–2270.

Kato M, Paranjape T, Muller RU, Nallur S, Gillespie E, Keane K, Esquela-Kerscher A, Weidhaas JB, Slack FJ (2009) The mir-34 microRNA is required for the DNA damage response in vivo in C. elegans and in vitro in human breast cancer cells. *Oncogene* **28**: 2419–2424.

Niemoeller OM, Niyazi M, Corradini S, Zehentmayr F, Li M, Lauber K, Belka C (2011) MicroRNA expression profiles in human cancer cells after ionizing radiation. *Radiat Oncol* **6**: 29.

Perez OD, Kinoshita S, Hitoshi Y, Payan DG, Kitamura T, Nolan GP, Lorens JB (2002) Activation of the PKB/AKT pathway by ICAM-2. *Immunity* **16**: 51–65.

Schetter AJ, Leung SY, Sohn JJ, Zanetti KA, Bowman ED, Yanaihara N, Yuen ST, Chan TL, Kwong DL, Au GK, Liu CG, Calin GA, Croce CM, Harris CC (2008) MicroRNA expression profiles associated with prognosis and therapeutic outcome in colon adenocarcinoma. *JAMA* **299**: 425–436.

Shiiba M, Nomura H, Shinozuka K, Saito K, Kouzu Y, Kasamatsu A, Sakamoto Y, Murano A, Ono K, Ogawara K, Uzawa K, Tanzawa H (2010) Down-regulated expression of SERPIN genes located on chromosome 18q21 in oral squamous cell carcinomas. *Oncol Rep* **24**: 241–249.

Wagner-Ecker M, Schwager C, Wirkner U, Abdollahi A, Huber PE (2010) MicroRNA expression after ionizing radiation in human endothelial cells. *Radiat Oncol* **5**: 25.

Weidhaas JB, Babar I, Nallur SM, Trang P, Roush S, Boehm M, Gillespie E, Slack FJ (2007) MicroRNAs as potential agents to alter resistance to cytotoxic anticancer therapy. *Cancer Res* **67**: 11111–11116.

Wu BH, Xiong XP, Jia J, Zhang WF (2011) MicroRNAs: new actors in the oral cancer scene. *Oral Oncol* **47**: 314–319.

Zhang Y, Yan LX, Wu QN, Du ZM, Chen J, Liao DZ, Huang MY, Hou JH, Wu QL, Zeng MS, Huang WL, Zeng YX, Shao JY (2011) miR-125b is methylated and functions as a tumor suppressor by regulating the ETS1 proto-oncogene in human invasive breast cancer. *Cancer Res* **71**: 3552–3562.

Supplementary Information accompanies this paper on British Journal of Cancer website (http://www.nature.com/bjc)

Lipocalin-2 is associated with radioresistance in oral cancer and lung cancer cells

MASASHI SHIIBA[1,2], KENGO SAITO[3], KAZUAKI FUSHIMI[1], TAKASHI ISHIGAMI[1], KEIJI SHINOZUKA[1], DAI NAKASHIMA[1], YUKINAO KOUZU[1], HIROFUMI KOIKE[1], ATSUSHI KASAMATSU[1], YOSUKE SAKAMOTO[1], KATSUNORI OGAWARA[1], KATSUHIRO UZAWA[1], YUICHI TAKIGUCHI[2] and HIDEKI TANZAWA[1]

Departments of [1]Clinical Molecular Biology, [2]Medical Oncology and [3]Molecular Virology, Graduate School of Medicine, Chiba University, Chuo-ku, Chiba 260-8670, Japan

Received November 12, 2012; Accepted December 21, 2012

DOI: 10.3892/ijo.2013.1815

Abstract. The aim of the present study was to identify a target molecule that could predict the efficacy of radiotherapy in oral squamous cell carcinoma (OSCC). We used DNA microarray analysis to identify differences in gene expression after X-ray irradiation. We compared the gene expression profiles between X-ray (8 Gy)-irradiated Ca9-22 cells (an OSCC-derived cell line) and unirradiated Ca9-22 cells. A total of 167 genes with a 2-fold higher level of expression induced by X-ray irradiation were identified. *Lipocalin-2* (*LCN2*) had the greatest increase in expression after X-ray irradiation, and it was categorized in a network that has cancer-related functions with the Ingenuity Pathway Analysis tool. Upregulated expression of *LCN2* mRNA was validated by real-time quantitative reverse transcriptase-polymerase chain reaction (qRT-PCR) analysis. When the *LCN2* gene was knocked down in OSCC cells (Ca9-22 and HSC-2) and lung cancer cells (A549) by using small interfering RNA, the radiosensitivity of these cells was enhanced. Our findings suggest that the overexpression of LCN2 is likely associated with radioresistance in oral cancer and lung cancer cells, and that LCN2 expression levels could be used to predict radioresistance. Thus, regulating the expression or function of LCN2 could enhance the radiation response, resulting in a favorable outcome of radiotherapy.

Introduction

Although radiotherapy for oral squamous cell carcinoma (OSCC) is effective in certain patients, some patients do not respond to radiotherapy. The discrepancy between responders and non-responders mostly depends on the radiosensitivity of tumor cells. Thus, it is crucial to determine the mechanism of radiosensitivity and to identify molecules that regulate radiotherapy responsiveness. Many studies have reported a correlation between gene expression and the response to radiotherapy (1-3). The products of these effector genes participate in a radiation-induced response (3-5), which includes necrosis, apoptosis, cell cycle arrest and DNA repair (5-7). In oral malignancies including OSCCs, cyclooxygenase-2 (COX-2) (8), surviving (9), DNA contact mutation of p53 (10), tumor suppressor homologue p63 (11), tongue cancer resistance-associated protein 1 (TCRP1) (12) and intercellular adhesion molecule 2 (ICAM2) (13) may be associated with radioresistance.

Lipocalins are a functionally diverse family of proteins that can bind to surface receptors and a variety of lipophilic substances. Lipocalins are upregulated in a number of pathological conditions and may function as transporters of essential factors (14) and regulators of cell homoeostasis and the modulation of the immune response (15). Lipocalin-2 (LCN2, also known as neutrophil gelatinase-associated lipocalin: NGAL), a member of the lipocalin family, exists as a 25-kDa monomer, a 46-kDa disulphide-linked homodimer and a 135-kDa disulphide-linked heterodimer with neutrophil gelatinase-B (16). LCN2 is thought to be an acute phase protein (17), the expression of which is upregulated in epithelial cells under diverse inflammatory conditions including appendicitis, inflammatory bowel disease and diverticulitis (18). Lipocalins affect cellular proliferation and differentiation, and may be involved in the development of carcinomas (19). Previous studies have reported that LCN2 is expressed in human colorectal cancer (18), pancreatic cancer cells, colorectal and hepatic tumors (20), and human ovarian cancer cell lines (21). In head and neck tumors, Hiromoto *et al* reported that LCN2 expression was strongly upregulated in well-differentiated OSCC tissues and moderately to weakly upregulated in moderately to poorly differentiated OSCC tissues, while its expression was weak or very weak in normal mucosa and leukoplakia (22). It was recently reported that the upregulation of LCN2 expression in human adenocarcinoma A549 cells was accompanied by apoptosis induced by several reagents and that the induction of LCN2 represents a survival response (14).

In the current study, we performed DNA microarray analysis to assess gene expression changes in OSCC cells after X-ray irradiation. The genes identified were subjected to network and gene ontology analysis, and functional analyses

Correspondence to: Dr Masashi Shiiba, Department of Clinical Molecular Biology, Graduate School of Medicine, Chiba University, 1-8-1 Inohana, Chuo-ku, Chiba 260-8670, Japan
E-mail: m.shiiba@faculty.chiba-u.jp

Key words: lipocalin-2, oral squamous cell carcinoma

were performed to clarify whether the candidate molecule is related to radioresistance by gene silencing.

Materials and methods

Cell lines and culture conditions. The human OSCC-derived cell lines Ca9-22, HSC-2 and the human lung cancer cells A549, were prepared for this study (Human Science Research Resources Bank, Osaka, Japan). The cells were maintained in Dulbecco's modified Eagle's medium F-12 HAM (Sigma Chemical Co., St. Louis, MO, USA) and supplemented with 10% heat-inactivated fetal bovine serum and 50 U/ml penicillin and streptomycin. All cultures were grown at 37˚C in a humidified atmosphere of 5% CO_2.

X-ray irradiation. The cells were irradiated using X-ray irradiation equipment (MBR-1520R-3, Hitachi, Tokyo, Japan) operated at 150 V and 20 mA with AL filtration at a dose of 2.1 Gy/min.

Isolation of RNA. Total RNA was extracted with TRIzol reagent (Invitrogen Life Technologies, Carlsbad, CA, USA) from irradiated and unirradiated cells 4 h after irradiation, according to the manufacturer's instructions. The quality of total RNA was determined by Bioanalyzer (Agilent Technologies, Palo Alto, CA, USA).

Preparation of cDNA. Total RNA was extracted using TRIzol reagent. Five micrograms of total RNA from each sample was reverse transcribed to cDNA using Ready-to-Go You-Prime first-strand beads (GE Healthcare, Buckinghamshire, UK) and oligo (dT) primer (Sigma Genosys, Ishikari, Japan), according to the manufacturer's protocol.

Hybridization of RNAs to oligonucleotide arrays. For microarray analysis, 4 h after irradiation (8 Gy) was selected as the time-point at which to monitor the early response of Ca9-22 cells to X-ray irradiation and to identify differentially expressed early genes that mediate cellular events such as DNA repair and apoptosis. We used Human Genome U133A Array GeneChip oligonucleotide arrays (Affymetrix, Santa Clara, CA, USA). This GeneChip, containing 22,283 probe sets, analyzes the expression level of over 18,400 transcripts and variants, including 14,500 well-characterized human genes. For hybridization, 20 μg of total RNA per sample was prepared according to the manufacturer's protocol (Affymetrix). Fragmented cRNA (15 μg of each) was hybridized to the Human Genome oligonucleotide arrays. The arrays were stained with phycoerythrin-streptavidin and the signal intensity was amplified by treatment with a biotin-conjugated anti-streptavidin antibody, followed by a second staining using phycoerythrin-streptavidin. The arrays stained a second time were scanned using the Affymetrix GeneChip Scanner 3000.

Analysis of microarray data. GeneChip analysis was performed based on the Affymetrix GeneChip Manual with Microarray Analysis Suite 5.0, Data Mining Tool 2.0 and Microarray Database software. The genes on the GeneChip were globally normalized and scaled to a signal intensity of 500. The Microarray Analysis Suite software used Wilcoxon's test to generate detected (present or absent) calls and used the calls to statistically determine if a transcript was expressed or not. After being filtered through a 'present' call ($P<0.05$), the expression data were analyzed using GeneChip Operating Software 1.1 (Affymetrix) and GeneSpring 6.1 (Silicon Genetics, Redwood City, CA, USA). Fold changes were calculated by comparing transcripts between irradiated Ca9-22 cells and unirradiated Ca9-22 cells. We identified 167 genes differentially expressed 2.0-fold or more by X-ray irradiation. The genes, which were identified by microarray analyses, were analyzed for network and gene ontology by Ingenuity Pathway Analysis (IPA) software (Ingenuity Systems, Mountain View, CA, USA) to identify networks of interacting genes. Gene accession numbers were imported into the IPA software. The genes were categorized based on location, cellular components, and reported or suggested biochemical, biologic and molecular functions using the software. The identified genes were mapped to the genetic networks available in the IPA database and then ranked by score. The score is the probability that a collection of genes equal to or greater than the number in a network could be achieved by chance alone. A score of 3 indicates that there is a 1/1,000 chance that the focus genes are in a network due to random chance. Therefore, scores of 3 or higher have a 99.9% confidence level of not being generated by random chance alone. This score was used as the cut-off for identifying gene networks.

Analysis of mRNA expression by real-time quantitative reverse transcriptase-polymerase chain reaction (qRT-PCR). Real-time qRT-PCR was performed to validate mRNA expression with a single method using a LightCycler FastStart DNA Master SYBR-Green 1 kit (Roche Diagnostics GmbH, Mannheim, Germany), according to the procedure provided by the manufacturer. Oligonucleotides used as primers were 5'-GCTGACTTC GGAACTAAAGGAGAA-3' and 5'-GGGAAGACGATGTG GTTTTCA-3' for LCN2 mRNA and 5'-CATCTCTGCCCCC TCTGCTGA-3' and 5'-GGATGACCTTGCCCACAGCCT-3' for *glyceraldehyde-3-phosphate dehydrogenase* (*GAPDH*) mRNA. Using LightCycler (Roche Diagnostics GmbH) apparatus, the experiment was carried out in a final volume of 20 μl of reaction mixture consisting of 2 μl of FirstStart DNA Master SYBR-Green I mix, 3 mM $MgCl_2$ and 1 μl of the primers, according to the manufacturer's instructions. Subsequently, the reaction mixture was loaded into glass capillary tubes and subjected to an initial denaturation at 95˚C for 10 min, followed by 45 rounds of amplification at 95˚C (10 sec) for denaturation, 62 to 64˚C (10 sec) for annealing, and 72˚C for extension. The transcript amount for the genes differentially expressed in the microarray analysis was estimated from the respective standard curves and normalized to the *GAPDH* transcript amount determined in corresponding samples.

Transfection of siRNAs in cells. SMARTpool siRNA targeting *LCN2* consists of four siRNAs targeting multiple sites on *LCN2* (*LCN2*-siRNAs). The sequences for *LCN2*-siRNAs are 5'-UGG GCAACAUUAAGAGUUAUU-3' (sense), 5'-PUAACUCUU AAUGUUGCCCAUU-3' (antisense), 5'-GAGCUGACUUC GGAACUAAUU-3' (sense), 5'-PUUAGUUCCGAAGUCAGC UCUU-3' (antisense), 5'-GAAGACAAAGACCCGCAAAUU-3' (sense), 5'-PUUUGCGGGUCUUUGUCUUCUU-3' (antisense), 5'-GAAGACAAGAGCUACAAUGUU-3' (sense) and 5'-PCAU

UGUAGCUCUUGUCUUCUU-3' (antisense) (On-Target plus SMARTpool, L-003679-00-0005, Human *LCN2*, NM005564). Positive and negative control siRNAs were purchased (Dharmacon, Lafayette, CO, USA). Two negative controls were used, vehicle control and siControl non-targeting siRNA pool (D-001206-13-20; siNT). Cyclophilin B (siControl cyclophilin B, siCyclo) was used as a positive silencing control to ascertain the transfection efficiency in each experiment. Cells were transfected with siRNAs using Dharma*FECT1* reagent (Dharmacon). Cells were plated in antibiotic-free Dulbecco's modified Eagle's medium F-12 HAM at a density of 200,000 cells/4 ml in 60-mm dishes. After 24 h, the cells were transfected with 100 nmol/l siRNA in Dharma*FECT1* reagent, according to the manufacturer's instructions. Briefly, 8 μl Dharma*FECT1* was diluted in 392 μl of serum-free medium and incubated at room temperature for 5 min. In a separate tube, 200 μl of 2 μmol/l siRNA was diluted in 200 μl of serum-free medium at room temperature for 5 min. Diluted Dharma*FECT1* (400 μl) was added to the diluted siRNA and the complex was incubated for 20 min at room temperature. The cells were washed with antibiotic-free Dulbecco's modified Eagle's medium F-12 HAM and 3.2 ml antibiotic-free Dulbecco's modified Eagle's medium F-12 HAM was added to each dish. siRNA + Dharma*FECT1* complex (800 μl) was added gently to the dish. The final concentration of siRNA was 100 nmol/l. Control cells were treated with medium only, the 100 nmol/l non-targeted siRNA (siNT negative control), and the 100 nmol/l cyclophilin B siRNA (positive silencing control). After 4 h of transfection, the medium of cells treated with *LCN2*-siRNA (siLCN2) and control cells was replaced with fresh medium, and cells were incubated at 37˚C in 5% CO_2 for 120 h before the experiments.

Western blot analysis. Cells were lysed in buffer [10 mM Tris base (pH 8.0), 400 mM NaCl, 3 mM $MgCl_2$, 0.5% Nonidet P-40 (Sigma), 100 mM phenylmethylsulfonyl fluoride and 0.01% protease inhibitor cocktail (Sigma)] at 4˚C for 10 min. Protein extracts were electrophoresed on 11% sodium dodecyl sulfate-polyacrylamide gel electrophoresis gels and transferred to polyvinylidene fluoride (PVDF) membranes (Bio-Rad, Hercules, CA, USA). Immunoblot PVDF membranes were washed with 0.1% Tween-20 in TBS, and affinity-purified mouse anti-human LCN2 monoclonal antibody (Santa Cruz Biotechnology, Santa Cruz, CA, USA) was added at 1:100 and incubated overnight at room temperature. PVDF membranes were washed again and incubated with a 1:5,000 of horseradish peroxidase-conjugated anti-mouse IgG Envision+ (Dako Japan Inc., Kyoto, Japan) as a secondary antibody for 2 h at room temperature. Finally, membranes were incubated with enhanced chemiluminescence (ECL)+ horseradish peroxidase substrate solution included in the ECL+ kit (GE Healthcare) and immunoblotting was visualized by exposing the membrane to Hyperfilm (GE Healthcare).

Cell survival assay. Cells were transfected as described previously with the vehicle, siNT and siLCN2. At 96 h after transfection, the cells were trypsinized, counted and the appropriate number of cells was plated in 60-mm dishes and allowed to attach for 24 h. After 24 h, the cells were irradiated (2, 4, 6, 8 Gy) and incubated for 8 to 10 days. The colonies were stained with crystal violet (Sigma Chemical Co.) and colonies of 50 cells or greater were counted. Clonogenic fractions of irradiated cells were normalized to the plating efficiency of unirradiated controls.

Cellular proliferation assay. To determine the effect of siLCN2 transfection on cell proliferation, Ca9-22 cells transfected with non-targeting or LCN2 siRNA were seeded in 12-well plates at a density of $1x10^4$ viable cells per well. At the indicated time point, cells were trypsinized and counted using a hemocytometer in triplicate samples.

Results

DNA microarray and network analysis. The gene expression profile in the irradiated OSCC-derived cell line Ca9-22, was analyzed with DNA microarray analysis. A total of 167 genes were overexpressed after X-ray irradiation (8 Gy) by at least 2-fold when compared with unirradiated Ca9-22 cells, while 14 genes were upregulated more than 5-fold (Table I).

We then investigated whether the 167 genes that were overexpressed by at least 2-fold interacted biologically by performing genetic network analysis with the IPA tool. Among these genes, 82 genes were mapped to six genetic networks in which functional relationships between gene products have been reported (Fig. 1). The six networks were highly significant and contained some common biological functions, such as cancer, cell death, cellular growth and proliferation (Table II). *LCN2*, which was mapped to network 2, had the greatest increase in expression after X-ray irradiation (Table I).

Validation of microarray data by real-time qRT-PCR analysis. To verify the gene expression identified in the DNA microarray analysis, real-time qRT-PCR was performed by using the same RNA that was used in the DNA microarray analysis. Consistent with the results of DNA microarray analysis, there was a significant increase in the expression levels of *LCN2* in X-ray irradiated Ca9-22 cells as compared with unirradiated Ca9-22 cells (Fig. 2). The data are expressed as the mean ± standard deviation (SD) of two independent experiments with samples in triplicate.

Functional analysis in siLCN2-tranfected cells. To determine whether LCN2 silencing contributes to radiation sensitivity, cells were transfected with siRNAs and screened for their ability to downregulate target protein expression. To ascertain that RNA inhibition conditions were optimal and transfection efficiency was satisfactory, *cyclophilin B* siRNA was used as a positive control in each experiment. In Ca9-22, HSC-2 and A549 cells transfected with cyclophilin B siRNA (siCyclo), the *cyclophilin B* protein level was reduced significantly as compared to the vehicle or siNT controls (siNT) (Fig. 3). LCN2 protein expression was examined by western blot analysis in Ca9-22, HSC-2 and A549 cells 120 h after transfection with siRNAs (Figs. 4-6). LCN2 protein levels in vehicle and siNT-transfected cells were comparable to that of LCN2 in non-treated cells. In addition, in cells transfected with 100 nmol/l siLCN2, the LCN2 protein level was reduced significantly as compared with the positive and negative control cells. These transfected cells were subjected to functional analysis to reveal the effect of LCN2 gene silencing in radiation response. Survival of Ca9-22, HSC-2 and A549 cells transfected with siLCN2 at 120 h decreased significantly ($P<0.01$, Student's

Table I. Differentially expressed genes (fold change >5).

Affymetrix no.	Symbol	Name	Fold change[a]
212531_at	*LCN2*	Lipocalin 2 (oncogene 24p3)	14.2
204580_at	*MMP12*	Matrix metalloproteinase 12 (macrophage elastase)	12.2
220026_at	*CLCA4*	Chloride channel, calcium activated, family member 4	11.6
220523_at	*FLJ22843*	Hypothetical protein FLJ22843	8.4
211708_s_at	*CESK1*	T-complex protein 1	8.2
211708_s_at	*C13orf10*	Chromosome 13 open reading frame 10	7.0
216697_at	*TRIO*	Triple functional domain (PTPRF interacting)	6.7
200831_s_at	*SCD*	Stearoyl-CoA desaturase (Δ^9desaturase)	6.6
214605_x_at	*GPR1*	G protein-coupled receptor 1	6.5
202815_s_at	*HIS1*	HMBA-inducible	6.1
213112_s_at	*SQSTM1*	Sequestosome 1	5.9
202828_s_at	*MMP14*	Matrix metalloproteinase 14 (membrane-inserted)	5.7
202820_at	*AHR*	Aryl hydrocarbon receptor	5.7
205660_at	*OASL*	2'-5'-oligoadenylate synthetase-like	5.0

[a]The fold changes in the genes after X-ray irradiation (8 Gy) cells compared with unirradiated cells.

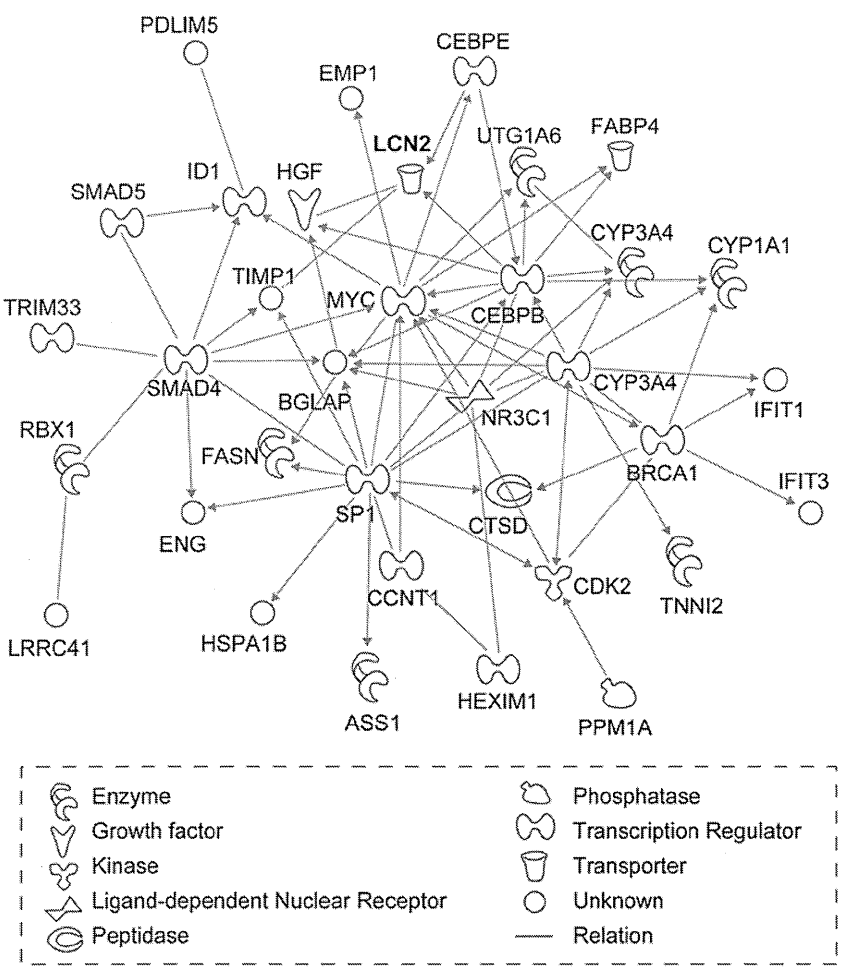

Figure 1. The network of molecules (including LCN2) categorized by IPA software. The identified network shows the classification of molecules and their interactions.

Table II. Genetic networks in the X-ray irradiated oral squamous cell carcinoma cells.

Network	Gene	Function	Score[a]
1	*ABCA1, ADI1, AHR, Ap1, CYP1A1, F12, FABP4, FADS1, FASN, FGA, FGB, FGG, G6PD, H3F3A, H3F3B, Histone h3, IDH1, LSS, Mmp, MMP1, MMP10, MMP12, MMP13, MMP14, N-cor, NID1, OLR1, SC5DL, SCD, SERPINA1, SREBF1, TBL1X, TBL1XR1, TESK1, TM7SF2*	Post-translational modification, genetic disorder, hematological disease	40
2	*ASS1, BGLAP, BRCA1, CCNT1, CDK2, CEBPB, CEBPE, CTSD, CYP1A1, CYP3A4, EMP1, ENG, FABP4, FASN, HEXIM1, HGF, HSPA1B, ID1, IFIT1, IFIT3, LCN2, LRRC41, MYC, NR3C1, PDLIM5, PPM1A, RBX1, SMAD4, SMAD5, SMARCA4, SP1, TIMP1, TNNI2, TRIM33, UGT1A6*	Cancer, gene expression, cellular growth and proliferation	30
3	*ADH1A, ADH1B, ADH1C (includes EG:126), AKR1C1, AKR1C2, alcohol dehydrogenase, CDKN2A, CEBPA, CFD, CTSA, DHRS9, E2F1, Fabp, FABP4, GLB1, GPRC5A, HIST1H2AC, HIST1H4H, HIST2H2AA3, INSIG1, JUNB, LCK, LNPEP, NEU1, NR2F2, NR4A1, PPARG, RETN, RXRA, SCD, SLCO1A2, SOX4, SPRR1B, SQSTM1, TK1*	Cancer, carbohydrate metabolism, digestive system development and function	30
4	*ACVR2A, BMP2, BMP6, BMPR2, BMPR1A, BMPR1B, CLK1, COL1A2, COL2A1, DSPP, EVL, FGF7, FGF10, FGFBP1, FYB, FYN, GPNMB, heparin, HGF, HIST1H2BH, IGFBP6, LPL, MDK, NFYB, PTPN1, RUNX2, SKAP1, SKAP2, SMAD5, SORT1, SOST, STAT1, TIMP3, WARS, ZNF323*	Cellular growth and proliferation, cellular development, connective tissue development and function	23
5	*AHR, ARNT2, CASP3, CAST, CDH1, CTSD, CTSK, Cyclin A, DNAJB1, E2F3, EFNA1, EPHA2, GLUL, HMGB1 (includes EG:3146), HSP90AA1, HSPA1A, IRF5, MAP3K5 PREDICTED, MAPK10, MAPK8IP3, PCLO, PFN1, PPP3R1, PTMA, PTPRF, PVRL1, PVRL3, RBBP5, SERPINB13, SKIL, TFE3, TNFRSF9, TNFSF9, TP53, TRIO*	Cell death, cellular growth and proliferation, cellular assembly and organization	21
6	*AR, Ca^{2+}, CACYBP, CALB1, CDC37, EXOC1, EXOC2, EXOC3, EXOC4, EXOC5, EXOC6, EXOC7, EXOC8, FYN, GSN, Hsp70, Hsp90, HSPA8, MAK, MBP, NOS3, OASL, PARK2, phosphatidylinositol, PIK3R1, RALA, S100A6, S100B, SIAH1, SNCA, SRC, THRB, TUBA1A, TUBB, VIL2*	Cellular function and maintenance, cell signaling, molecular transport	9

Underlining indicates genes identified by microarray analysis. [a]A score >3 was considered significant.

t-test) after 2, 4, 6 and 8 Gy of irradiation compared with that of corresponding cells treated with siNT (Figs. 4-6). To determine the effect of siLCN2 transfection on cell proliferation, cellular proliferation assay was performed. The data showed no significant effect by siLCN2 transfection on cellular proliferation in Ca9-22 cells (Fig. 7).

Discussion

Although radiotherapy is considered an effective treatment choice in patients with OSCC, the outcome is not favorable in certain cases. The difference in the outcome mainly depends on the radiosensitivity of tumor cells. Although a set of human genes related to radiosensitivity has been identified (23-29), the

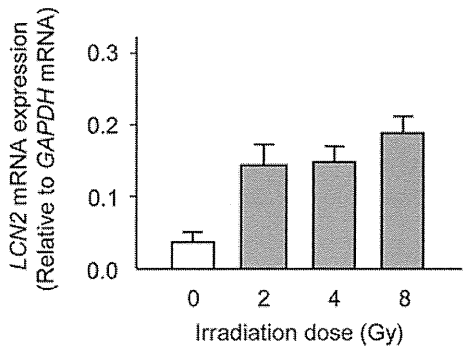

Figure 2. Quantification of *LCN2* mRNA levels by real-time qRT-PCR analysis of irradiated (2, 4 and 8 Gy) Ca9-22 cells. The expression of *LCN2* mRNA was upregulated in irradiated Ca9-22 cells as compared to unirradiated Ca9-22 cells.

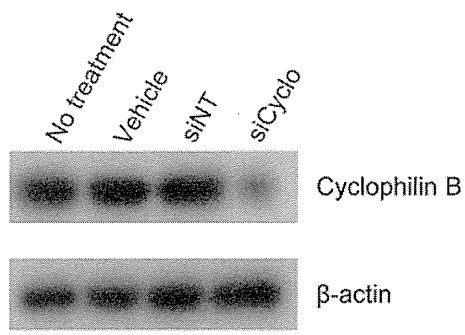

Figure 3. Western blot analysis of cyclophilin B protein in Ca9-22 cells. The cells were transfected with vehicle, siNT, siCyclophilin B (siCyclo) and analyzed after 120 h. The expression of cyclophilin B was diminished in cells transfected with siCyclo. There was no change in the cyclophilin B expression of cells transfected with siNT (negative control siRNA). β-actin was used as a loading control.

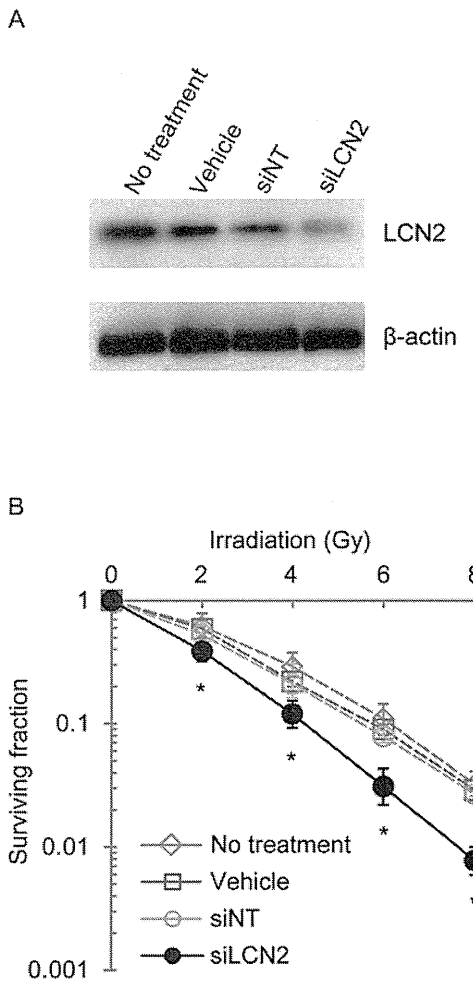

Figure 4. Functional analysis of siLCN2-transfected Ca9-22 cells. (A) Decreased expression of LCN2 protein in siLCN2-transfected Ca9-22 cells was validated by western blot analysis. (B) Survival of siLCN2-transfeced Ca9-22 cells was significantly decreased after 2, 4, 6 and 8 Gy of radiation as compared with that of siNT-transfected cells (*P<0.01, Student's t-test).

detailed mechanism of radioresistance remains unknown. Thus, the present study aimed to identify molecules that control the response to radiotherapy in OSCC. We identified 167 genes that were upregulated by X-ray irradiation (8 Gy) in Ca9-22 cells by using DNA microarray analysis. We used the IPA tool to analyze the functional networks and gene ontology of these genes, and we detected six genetic networks that were each characterized by different representative functions (Table II). Among the genes, *LCN2*, which mapped to network 2, had the greatest increase in expression after X-ray irradiation (Table I). A variety of functions of the LCN2 protein has been reported. These functions include the transport of fatty acids and iron (30,31) and the modulation of inflammatory responses (32). A recent study reported that *LCN2* expression was upregulated accompanied with apoptosis induced by several reagents in human adenocarcinoma A549 cells and that the induction of *LCN2* represents a survival response (14). Roudkenar *et al* detected the upregulation of LCN2 expression in HepG2 cells after the administration of X-rays or H_2O_2 (33). These studies suggest that LCN2 defends cells against extracellular stimuli and facilitates cell survival. In the current study, the expression of *LCN2* was significantly upregulated by X-ray irradiation (Fig. 2), and *LCN2* gene silencing enhanced the radiosensitivity of OSCC cells and lung cancer cells (Figs. 4-6). Thus, LCN2 should also have supported the survival of irradiated cells in the present study. The biological activity of LCN2 is not cell-specific because the same effect was observed in two different OSCC-derived cell lines and a lung cancer cell line.

Park *et al* reported that phosphoinositide 3-kinase (PI3K)/Akt mediates the interleukin-3-regulated expression of 24p3, the mouse analogue of LCN2, in hematopoietic cells (34). Thus, the PI3K/Akt pathway might be closely related to LCN2 expression in solid tumors. We previously reported that the downregulation of ICAM2 expression by siRNA enhanced the radiosensitivity of OSCC cells with an increased apoptotic phenotype via phosphorylation of Akt (13). These studies indicate that the PI3K/Akt pathway may play a crucial role in the radiosensitivity of OSCC and that LCN2 might be involved in this mechanism.

The current study indicates for the first time that LCN2 is related to radioresistance. Various molecules have been reported to be associated with the radiotherapy response of malignant tumors of the head and neck. p53 DNA contact mutation (10), COX-2 (8), p63 (11) and TCRP1 (12) induced radioresistance, while high survivin expression (9) and downregulated expression of ICAM2 (13) enhanced radiosensitivity. However,